Journal of Marine Research, 56, 1125–1161, 1998

Observations of temporal changes of tritium-^{3}He age in the eastern North Atlantic thermocline: Evidence for changes in ventilation?

by Paul E. Robbins[1,2] and William J. Jenkins[1,3]

ABSTRACT

A compilation of fifteen years of tritium and ^{3}He measurements is used to examine the ventilation of the eastern North Atlantic subtropical gyre with specific emphasis on the temporal character of the tracer age field. A multivariate regression analysis in the form of a spatiotemporal Taylor expansion is applied to observations interpolated onto isopycnal surfaces. The time-dependent component of the tracer age field is found to be statistically significant, explaining approximately 10% of the variance of the tracer age observations in the upper thermocline ($\sigma_\theta = 26.5$) and increasing to roughly 50% of the variance in the lower thermocline ($\sigma_\theta = 27.0$). The observed transient tracer age increases over the 15 years of observations with the fractional rate of change of the age field varying between 2% and 5% per year. The largest observed changes occur on the deepest, most slowly ventilated isopycnal surfaces. The second derivative of the tritium-^{3}He age with time suggests that the tracer age field may be approaching a steady state.

If tritium-^{3}He age is interpreted as a true measure of the advective ventilation age, the temporal changes in age would imply a slackening of the ventilation of the lower main thermocline of greater than 50% from the late 1970's to the early 1990's. However, consideration of the full advective-diffusive balance of tritium-^{3}He age reveals that the changes in tracer age field represent a time-dependent adjustment of the transient tracer concentrations in conjunction with a steady local circulation field. Integral approximations of the upstream evolution of the tracer field also fail to demonstrate evidence for decadal changes in ventilation. The integral balance along the path of subduction yields an improved estimate of the true ventilation age based on the temporal tendency of the age field along the path of ventilation. An approximation of this integral suggests that actual ventilation ages can be up to 40% larger than the measured tracer age in the deeper portions of the North Atlantic thermocline. Proper accounting of the time-dependent biases of the tracer age dating technique are a prerequisite for examining transient tracer measurements for evidence of changes in the physical ventilation of the upper ocean.

1. Introduction

Observations of transient tracers offer a unique opportunity to observe directly the ventilation of the world's oceans. Anthropogenic tracers deposited into the surface ocean

1. Woods Hole Oceanographic Institution, Woods Hole, Massachusetts, 02543, U.S.A.
2. Present address: Scripps Institution of Oceanography, University of California San Diego, La Jolla, California, 92093, U.S.A.
3. Present address: Southampton Oceanography Centre, Empress Dock, Southampton SO14 3ZH, United Kingdom.

penetrate the ocean interior by both subduction and deep convection. While transient tracers offer a clear qualitative picture of these ventilation pathways, quantitative interpretation is complicated by the same property that leads to their utility: concentrations vary over both space and time. Direct oceanic observations are limited and most property distributions are severely undersampled in space and time. Frequently, oceanic data are interpreted under an assumption of steadiness so that observations gathered at different points in time may be combined to form a single picture of the spatial distribution of properties. The difficulties of interpreting an undersampled data set are amplified for transient tracers since an assumption of steadiness is clearly invalid. Additionally, quantitative interpretation of interior tracer concentrations typically requires accurate knowledge of the history of the surface boundary condition concentration (Wunsch, 1988). Such histories are rarely measured directly and, rather, must be reconstructed from records of anthropogenic production rates combined with models of delivery to the ocean and constrained with available direct observations (Dreisigacker and Roether, 1978; Doney *et al.,* 1993).

To circumvent some of the difficulties associated with quantitative analysis of transient tracer concentrations, many investigators have proposed transforming tracer concentration measurements into a tracer age estimate (Jenkins and Clarke, 1976; Roether and Fuchs, 1988; Thiele and Sarmiento, 1990; Weiss *et al.,* 1985; Warner *et al.,* 1996). The age of a parcel is defined as the elapsed time since the water was resident in the surface mixed layer. In many cases, simultaneously measured transient tracer concentrations can be manipulated to form an estimate of the water's age. For example, tritium introduced to the surface ocean as tritiated water radioactively decays to form ^{3}He with a half life of 12.43 yr (Unterweger *et al.,* 1980). Dissolved helium in the surface mixed layer quickly equilibrates with the atmosphere. Therefore, for fluid beneath the surface mixed layer, measurements of ^{3}He concentrations above the equilibrium value are interpreted to have derived from the radioactive decay of tritium. The observed ratio of the two tracers defines a tritium-^{3}He age, τ:

$$\tau = \frac{1}{\lambda} \log_e \left(1 + \frac{^3\mathrm{He}}{^3\mathrm{H}} \right), \tag{1}$$

where λ is decay constant of tritium.

A diagnostic such as tritium-^{3}He age offers two potential advantages over actual tracer concentrations. Firstly, age is defined to be zero in surface waters so complications arising from changing boundary conditions are avoided. Secondly, since age is a property of the flow field, the spatial distribution of age is expected to be steady for a steady-state circulation field. The latter feature offers a great benefit for sparsely measured chemical species since the hypothesis of a steady-state tracer diagnostic allows for observations collected at different times to be simply combined to form a single estimate of the field.

This simple interpretation of age based on ^{3}He and tritium observations is complicated, however, since the accuracy of an age estimate diagnosed from transient tracer concentra-

tions may be affected by internal mixing within the ocean (Jenkins, 1987; Musgrave, 1990; Thiele and Sarmiento, 1990). The validity of tracer age dating rests on the assumption that after subduction, the chemical constituents of water parcels evolve as a "closed system." That is, the measured tritium and excess ^{3}He concentration is the direct result of the decay of the tritium content of the water and is not modified by mixing with the tritium and ^{3}He concentrations of surrounding waters. The assumption that the tracers concentrations are not affected by mixing with surrounding waters is almost certainly not satisfied in the ocean. Thiele and Sarmiento (1990) have explored the impact of mixing on diagnosed tracer age in idealized numerical simulations of thermocline ventilation. They found that the effects of mixing may be large for the ventilation of tracers in areas of intense recirculation (such as near the western boundary currents). In contrast, their simulations suggest that mixing results in only a minimal distortion of the diagnosed age field from transient tracer measurements in the well ventilated regions of the subtropical thermocline.

Previous analyses of tritium-^{3}He age observations in the North Atlantic Ocean appear to support the conclusions of the numerical simulations of Thiele and Sarmiento (1990). Specifically, Roether (1989) presents evidence suggesting a near steady-state of the tritium-^{3}He age field in the eastern North Atlantic thermocline: hydrographic stations occupied three years apart suggest an upper limit for temporal changes of tritium-^{3}He age in this well-ventilated region of the ocean to be 0.15 yr/yr. In contrast to the eastern North Atlantic, a 14 year time series of tritium and ^{3}He measurements at Bermuda (Jenkins, 1991), a region typified by recirculated flow south of the Gulf Stream, reveal substantial changes in the diagnosed tritium-^{3}He age value. At Bermuda, the observed tracer ages change at rates of approximately 0.5 yr/yr in the middle and lower levels of the thermocline.

A direct interpretation of the "true" advective ventilation age based on the tracer age diagnostic necessarily requires that the tracer age field be steady if the ocean circulation is unchanged. Alternatively if the underlying circulation field is seen to change over time, the tracer age distribution should likewise alter in lockstep. The present paper utilizes 15 years of tritium and ^{3}He measurements in the subtropical eastern North Atlantic to re-examine the steadiness of the tracer age. Unlike the time series of measurements at Bermuda, tracer observations in the eastern North Atlantic have not been collected on a regular schedule or at a constant location. Therefore, examination of any temporal trends in the tracer age field requires an analysis which extracts the time-dependent signal from any spatial variations in the tracer fields. This paper uses a multivariate regression analysis to extract the large-scale spatiotemporal structure from the historical data set of tritium and ^{3}He measurements in the eastern North Atlantic. Whereas previous analysis of a time series of tritium and ^{3}He measurements at Bermuda can only examine the temporal component in the field, the present work simultaneously determines both the spatial and temporal structure of the tracer field allowing for more complete interpretation of possible observed changes.

The interior, southward flowing limb of the anticyclonic wind-driven gyre occupies the eastern subtropical North Atlantic. The combination of Ekman convergence and net

surface buoyancy exchange lead to southward subduction of surface waters from the winter mixed layer into the permanent thermocline (Marshall *et al.,* 1993). In addition to the generally southward flow from surface outcrops, the eastern subtropical gyre is fed by waters from the eastward flowing Azores Current (Klein and Siedler, 1989) which transports water from the Gulf Stream extension. The predominant subtropical mode water of the North Atlantic is Eighteen Degree Water ($\sigma_\theta \approx 26.5$) (Worthington, 1959) formed south of the Gulf Stream and to lesser extents in the eastern Atlantic near Madeira (Siedler *et al.,* 1987). Isopycnal surfaces composing the main thermocline with density anomaly greater than 26.5 outcrop into the surface winter mixed layer of the eastern Atlantic in the region north of the Azores Current. Isopycnal surfaces less dense than $\sigma_\theta \approx 27.2$ outcrop south of the zero line of the wind-stress curl and thus intersect the surface mixed layer within the domain of the traditionally defined anticyclonic subtropical gyre (Isemer and Hasse, 1987). The focus of the analysis of this paper will be on these density anomaly classes (26.5–27.2) which outcrop within the northern domain of the subtropical circulation.

The remainder of the paper is structured as follows. Section 2 reviews the spatiotemporal distribution of tritium and ^{3}He observations in the upper North Atlantic. Section 3 uses a multivariate regression analysis to extract the large-scale temporal changes in the tracer age field in the thermocline. Significant trends are found in the diagnosed age, especially in the lower thermocline. Section 4 examines hypotheses questioning the interpretation of the temporal trends in tracer age. Specifically, are the changes in tritium-^{3}He age evidence for decadal variability in the ventilation of the thermocline? Two separate facets of the change of tracer age are examined. The first, an advective-diffusive balance of the local tritium-^{3}He age budget, results in estimates of the local isopycnic velocity field and its rate of change over time. The second, a consideration of the integral balance of the Lagrangian increase in tracer age along the pathway of ventilation, yields estimates of the stability of the ventilation upstream of the location of the tracer observations. Additionally, the integral balance provides a means for more accurately estimating the true advective ventilation age from the observations of tritium-^{3}He age and its time rate of change. Section 5 summarizes the results and discusses the implications for interpretation of transient tracer age fields.

2. The spatiotemporal distribution of tritium-^{3}He age measurements in North Atlantic

Observations of tritium and ^{3}He in the North Atlantic Ocean extend back to the early 1970's. Figure 1 displays the distribution of hydrographic stations in the North Atlantic at which both tritium and ^{3}He were measured. Some survey programs, such as the Transient-Tracers in the Ocean (TTO) entailed basin-wide sampling while others, such as some of the cruises associated with the Subduction Experiment, consist of many closely-spaced stations in a small region. Although the survey patterns encompass a wide range in space and time, the eastern subtropical Atlantic stands out as the best observed portion of this basin. Indeed, in terms of ^{3}He and tritium measurements, the eastern subtropical Atlantic is

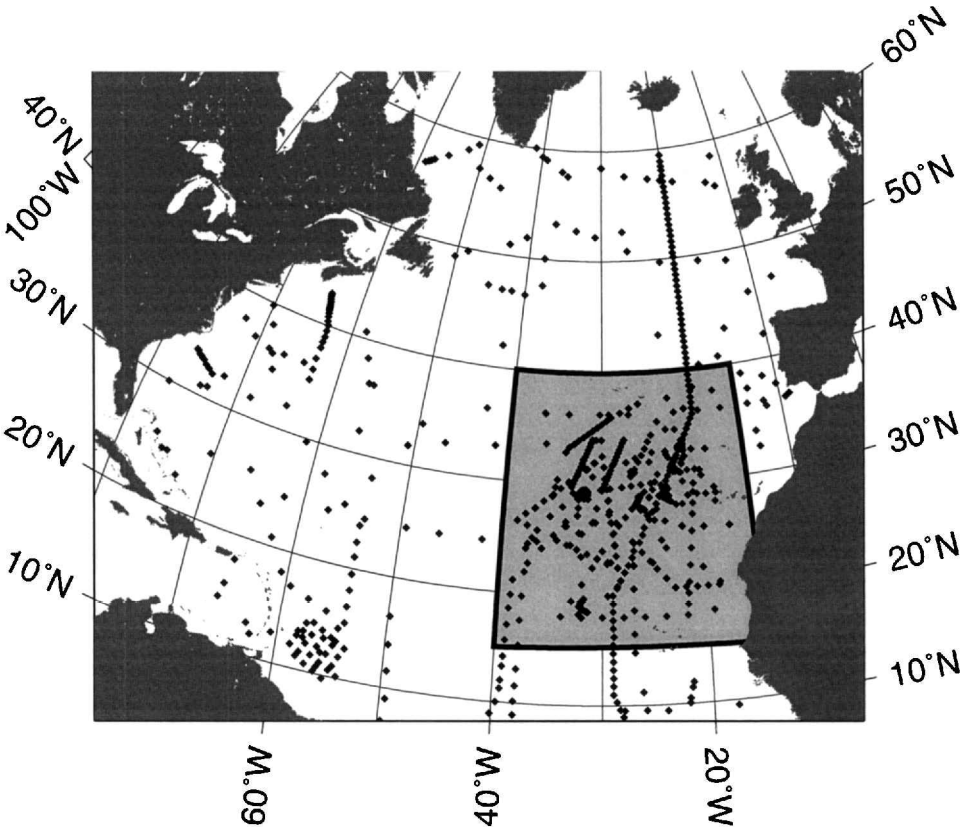

Figure 1. Distribution of hydrographic stations in the North Atlantic with both tritium and ^{3}He measurements in the density anomaly range 26.5–27.2. The geographic domain of data used in this analysis is indicated by the light shaded box in the eastern Atlantic.

the most thoroughly measured region in the entire world ocean. The analysis of this paper will be confined to this densely sampled subregion of the North Atlantic, roughly from 15–40N and 15–40W.

Table 1 summarizes the information pertaining to the research cruises from which the data for this analysis are drawn. The majority of the data comes from the archives of measurements performed by the Helium Isotope Laboratory at Woods Hole. These data are supplemented with measurements performed on the German vessel F/S *Meteor* (cruises 56, 64, and 69) as reported in Fuchs (1987). The combination of tritium and ^{3}He measurements from all the individual survey programs provides a unique set of transient tracer observations. The 15 hydrographic surveys span 15 years and include 496 stations with both tritium and ^{3}He measurements. The data set incorporates a total of 4076 samples processed for tritium analysis and 3595 for ^{3}He with the greatest number of samples collected in the early 1980's and early 1990's. Owing to differing cruise objectives, the spatial coverage,

Table 1. Summary of cruises measuring ^{3}H and ^{3}He in the eastern North Atlantic used in this analysis. The listed number of measurements represents only data for samples within the domain of the study. The first column lists either the program or ship and cruise number of the survey. Additional notes designating cruise information are added in parenthesis.

Ship/cruise	Year	Stations	^{3}H samples	^{3}He samples
R/V *Oceanus*-52	1978	13	184	107
R/V *Atlantis II*-107 (β-Triangle 1979)	1979	44	420	380
R/V *Oceanus*-79 (β-Triangle 1980)	1980	18	72	72
F/S *Meteor*-56	1981	15	306	119
Transient-Tracers in the Ocean (TTO)	1981	54	524	448
R/V *Atlantis II*-109	1981	37	306	261
Tropical Atlantic Survey (TAS)	1983	29	311	139
F/S *Meteor*-64	1983	7	18	69
F/S *Meteor*-69	1984	8	41	71
R/V *Endeavor*-143 (Pilot Subduction)	1986	60	446	421
R/V *Oceanus*-202	1988	13	189	180
R/V *Oceanus*-240/2 (Subduction Mesoscale)	1991	69	230	283
R/V *Oceanus*-250/3 (Subduction Seasoar)	1992	5	82	61
R/V *Oceanus*-254/4 (Subduction Large-scale)	1992	57	564	619
R/V *Oceanus*-258/3 (Subduction Mesoscale)	1993	67	383	365

both geographically and with depth, is far from uniform over the 15 years of coverage. While some cruises surveyed the large-scale structure of the subtropical gyre, others sampled only small regions, albeit with fine-resolution.

Likewise, the vertical resolution of the hydrographic sampling varied depending on the intent of the survey. Figure 2 shows the total number of samples collected in each year for selected isopycnal layers within the main thermocline. The shallower portion of the thermocline ($\sigma_\theta < 26.8$) was sampled much more intensively during the Subduction Experiment (1991–1993) than at anytime prior to 1990 (Table 2 summarizes the mean properties of selected isopycnals in the region of the analysis). In the lower portion of the thermocline however ($\sigma_\theta > 26.9$), the data coverage is more uniform in time. In general the best sampling coverage over the time span of the data record is in the central thermocline (between $\sigma_\theta = 26.4$ and $\sigma_\theta = 27.1$) with the periods of greatest coverage centered around 1981 and 1992. Other cruises with fewer measurements supplement these "data-rich" periods so that gaps in the temporal record never exceed three years.

3. The large-scale trends of the tritium-^{3}He age field in the eastern North Atlantic

The varied spatial and temporal coverage of the transient tracer fields in the eastern Atlantic precludes a direct estimate of changes in the tracer age field as has been done with the Bermuda time series (Jenkins, 1991). Differences observed from cruise to cruise reflect a possible aliasing of temporal changes by spatial gradients of the large-scale structure of the tracer fields. Nonetheless, inspection of the data suggests that temporal trends in the

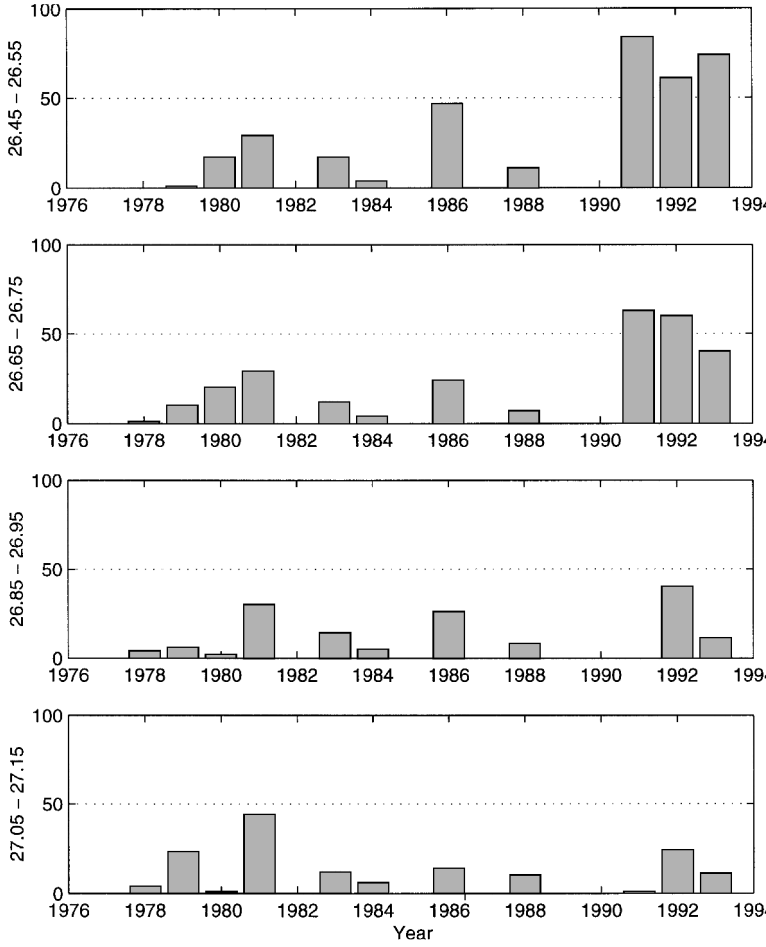

Figure 2. Temporal distribution of tritium and ^{3}He measurements in the main thermocline of the eastern Atlantic as a function of density class. Bars indicate the number of hydrographic samples per year analyzed for both ^{3}He and tritium.

tritium-^{3}He age field are sufficiently large to stand out above the spatial effects. Doney *et al.* (1997) compared data collected on a meridional section in 1988 with observations from the early 1980's and report an apparent shift in tritium-^{3}He age values in the lower thermocline ($\sigma_\theta > 26.85$). Qualitative changes in the tracer age field become even more apparent using the data collected in the early 1990's. Figure 3 compares the diagnosed tritium-^{3}He age on the isopycnal surface $\sigma_\theta = 27.0$ as a function of latitude based on measurements in both 1981 and 1992. A large meridional gradient of tracer age is evident, with age decreasing toward the surface outcrop to the north. Comparison of the data from the two separate years suggests a large, overall increase in the age south of 30N. It is unlikely that the large apparent temporal change arises from the spatial differences in the

Table 2. Summary of isopycnal surfaces used in analysis. Mean pressure, salinity and potential temperature of each density surface at 30W, 30N are evaluated from the climatological atlas of Lozier *et al.* (1995).

σ_θ (kg/m^{-3})	Pressure (dbar)	Θ (C)	Salinity (psu)
26.4	93	18.00	36.50
26.5	131	17.40	36.41
26.6	178	16.63	36.29
26.7	226	15.74	36.15
26.8	287	14.80	36.01
26.9	360	13.83	35.87
27.0	444	12.82	35.73
27.1	540	11.83	35.61
27.2	640	10.95	35.53
27.3	732	10.23	35.49

survey patterns of the separate years: the 1992 data span much of the longitudinal domain of the study and reveal only weak zonal gradients. The multivariate regression analysis of the following section will show that the observed temporal changes cannot be attributed to differences in geographic sampling.

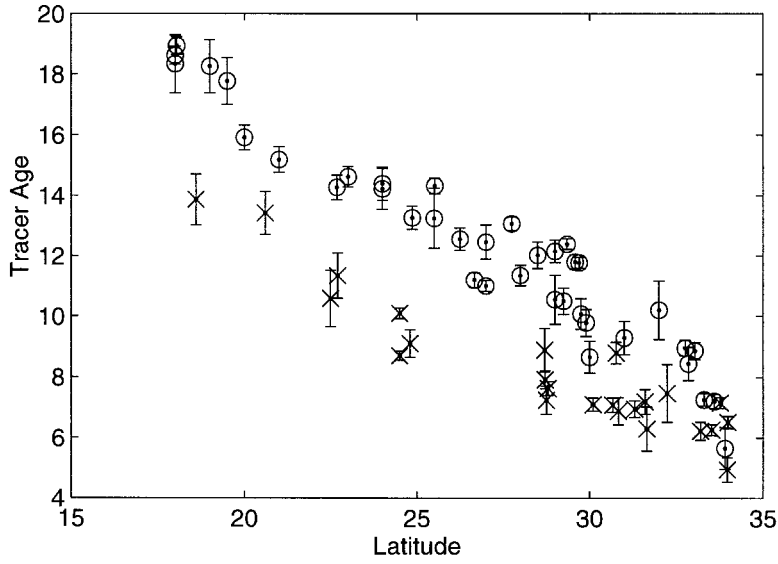

Figure 3. Tritium-^{3}He age observations on σ_θ = 27.0 at two different years. Samples collected in 1992 are indicated by an 'o' while those from 1981 are represented with an 'x.' Error bars represent uncertainty to the combined analytic and interpolation errors. All observations between 15W and 40W are plotted.

a. Multivariate regression analysis

Estimation of temporal trends in the mixed space and time data set of tritium-^{3}He age measurements in the eastern Atlantic requires a technique to simultaneously account for both spatial as well as temporal changes in the structure of the large-scale field. The combined space-time analysis is required so that changes in the observed age field due to the different geographic tracks of the survey cruises are not misinterpreted as temporal trends. This paper uses a multivariate regression analysis to simultaneously estimate the spatial gradients of the tritium-^{3}He age field as well as the temporal changes. The analysis is applied to the observed distribution of tritium-^{3}He age on isopycnal surfaces. The choice of an isopycnal coordinate system reflects prior analyses of transient tracer distributions which determined that the penetration of properties into the interior thermocline appears to be largely confined to transport along isopycnal surfaces (Rooth and Östlund, 1972; Jenkins, 1980; Fine *et al.,* 1981; Sarmiento *et al.,* 1982; Fine *et al.,* 1987).

The application of a multivariate regression analysis to the tritium and ^{3}He data assumes that the oceanic field of tritium-^{3}He age can be well described by a low-order polynomial expansion. This type of analysis is only capable of capturing those portions of the data which vary slowly in both space and time. If the variability of the tritium-^{3}He age field is mostly characterized by high frequency spatial and temporal scales, a regression analysis based on polynomial expansions will provide only a poor estimate of the structure of the true oceanic distribution. It is most likely, however, that the regional structure of the tritium-^{3}He age field in the main thermocline do vary slowly in both space and time.

i. Treatment of data. The tritium and ^{3}He data are linearly interpolated on a station-by-station basis onto surfaces of constant potential density spanning the range of the main thermocline. Each individual estimates of ^{3}He and ^{3}H on the selected isopycnal surface is assigned an uncertainty, $\sigma_{interpolation}$, based on proximity to bottle depths and curvature of the profile with respect to density (Robbins, 1997). The interpolated tritium and ^{3}He concentrations are then used to calculate tritium-^{3}He age. The resulting uncertainty assigned to each tritium-^{3}He age estimate is therefore based on both analytic and interpolation errors. The total number of tritium-^{3}He age data points on each isopycnal surface varies from near 300 on $\sigma_\theta = 26.5$ to 90 on $\sigma_\theta = 27.2$. Further decrease in sample density with depth precludes extending the analysis below $\sigma_\theta = 27.3$.

Tracer age is expected to have large gradients along the path of the mean flow. Because of the significant spatial gradients, the stirring of the tracer field by mesoscale variability may lead to substantial spatial and temporal variations on the scales of the eddy field. Since the multivariate regression of the tracer age field attempts to capture only the large-scale structure of the spatiotemporal distribution of the observations, the effects of mesoscale granularity are best accounted for by including them as "noise" in the observations. The magnitude of the deviations introduced by mesoscale stirring should scale as a mixing length times the mean gradient (Armi and Stommel, 1983; Jenkins, 1987; Joyce and

Jenkins, 1993):

$$\tau' = l' |\nabla \tau| \tag{2}$$

where l' is the mixing length. Adopting a mixing length of 100 km[4] and a large-scale gradient based on the minimum and maximum age value observed on each isopycnal, Eq. 2 can be used to estimate the uncertainty in measurements of the large-scale age field, $\sigma_{mesoscale}$, due to mesoscale eddy variability.

ii. Statistical test of steadiness. Assuming, for the moment, the tracer age is steady, we can represent the isopycnal tracer age field as a Taylor expansion about the center of the geographic domain ($\overline{longitude}$, $\overline{latitude}$):

$$\tau_{observed} = F(X, Y) = \overline{\tau} + \tau_x X + \tau_y Y + \tau_{xx} X^2 + \tau_{yy} Y^2 + \tau_{xy} XY + \cdots \tag{3}$$

where

$$X = [longitude - \overline{longitude}],$$
$$Y = [latitude - \overline{latitude}]$$

and the subscripts on the τ terms represent spatial derivatives. Given observations of τ at locations (X, Y), Eq. 3 forms a multivariate model of the observations as function of geographic position. The regressor variables are the mean tracer age ($\overline{\tau}$) and the spatial derivatives of the age field (τ_x, τ_y, . . .). The optimum order of the regression in Eq. 3 is chosen to obtain a model statistically consistent with the data (Anderson, 1984).

If, on the other hand, the structure of the large-scale tritium-^{3}He age field is changing over time, the steady-state Eq. 3 will fail to capture the variability of the time dependent portion of the observations. In this case we might consider representing the age field as an expansion in the temporal as well as the spatial domain:

$$\begin{aligned}\tau_{observed} = F(X, Y, T) = \overline{\tau} + \tau_x X + \tau_y Y + \tau_t T + \tau_{xx} X^2 \\ + \tau_{yy} Y^2 + \tau_{tt} T^2 + \tau_{xy} XY + \tau_{xt} XT + \tau_{yt} YT + \cdots\end{aligned} \tag{4}$$

where

$$T = [time - \overline{time}].$$

As in the spatial expansion, the temporal expansion is centered around a mid-point in time of the data set: *time*.

4. A length scale of 100 km is adopted from published estimates of length scale based on observed mesoscale distribution of tracer fields (Armi and Stommel, 1983; Jenkins, 1987; Joyce and Jenkins, 1993). The along-track auto-correlation function from TOPEX/POSEIDON altimeter data in the eastern Atlantic suggests a comparable length scale (Stammer and Böning, 1996). Integral length scales determined from float dispersal in this region are smaller with estimates ranging from 20 to 80 km (Böning, 1988).

iii. Weighting the multivariate regression. Least-squares solutions for multivariate regression models (such as Eq. 3 or 4) can be obtained by casting the algebraic equations into matrix notation (Menke, 1984):

$$\tau = \mathbf{E} * \mathbf{m} \tag{5}$$

where τ is the observed tracer age, $\mathbf{E}$ is a matrix of the regressor values containing the position and date of observation and $\mathbf{m}$ is a vector of the model coefficients, in this case the spatial and temporal derivatives of the tritium-^{3}He age field. The solution for model coefficients is then:

$$\mathbf{m} = (\mathbf{E}'\mathbf{W}\mathbf{E})^{-1}\mathbf{E}'\mathbf{W}\tau \tag{6}$$

where primes indicate the transpose operator and the weighting matrix $\mathbf{W}$ possesses diagonal elements proportional to the inverse of the data uncertainties:

$$\mathbf{W}_{ii} = [(\sigma_{interpolation})^2 + (\sigma_{mesoscale})^2]^{-1}. \tag{7}$$

The uncertainty of each observation of tritium-^{3}He age includes both interpolation errors and uncertainty due to mesoscale graininess (Eq. 2). Typical values of $\sigma_{interpolation}$ are less than 0.3 yr. The magnitude of $\sigma_{mesoscale}$ varies from 0.4 yr in the upper thermocline ($\sigma_\theta = 26.4$) to 1.2 yr on the densest isopycnals used in this analysis ($\sigma_\theta = 27.2$). The revised uncertainty estimate of Eq. 7 sets a minimum noise level for each estimation of tracer age regardless of the precision of the analytic measurements or smallness of the interpolation error.

In general, adding more regressor variables, such as including regressions against the time of observations, will always increase the ability of the regression model to reproduce the observations. Appendix A describes the statistical tests employed in this study to determine if the regression model based on a temporal expansion (Eq. 4) yields statistically significant improvement over the steady-state (Eq. 3) regression.

b. Application of multivariate regression model to tritium-^{3}He age observations

i. Variance of observations explained by regression analysis. The multivariate regression models based on polynomial expansions are applied to the record of tritium-^{3}He age observations on isopycnal surfaces spanning the main thermocline in the eastern North Atlantic. Table 3 summarizes the ability of regression models of differing order to explain the observed variance of the data. In the upper portion of the main thermocline, the spatiotemporal regression analysis can explain approximately one half of the large-scale variation of the observations. The explanatory power of the analysis increases to over 90% in the lower reaches of the thermocline.

As expected, regression analyses with a larger number of regressor variables, either a higher order polynomial expansion or inclusion of temporal terms, capture more of the variance of the tritium-^{3}He age observations. Application of an *F*-test statistic (Appendix) reveals that the addition of temporal terms in the polynomial expansion leads to statisti-

Table 3. Summary of percentage of variance of observations explained by multivariate regression analysis employing only spatial expansion terms (latitude and longitude) and both temporal and spatial expansion terms. For each class of model, the table displays the variance for models which truncate the Taylor expansion at the linear expansion terms (first order), quadratic terms (second order) and cubic terms (third order).

	Only spatial			Spatial and temporal		
	Order of expansion			Order of expansion		
σ_γ (kg m^{-3})	First	Second	Third	First	Second	Third
26.4	38.4	43.7	43.6	38.9	50.5	51.5
26.5	51.2	52.1	53.0	55.9	61.5	63.4
26.6	43.5	45.0	45.4	54.2	56.6	61.0
26.7	39.9	41.4	44.0	61.8	64.1	65.7
26.8	46.1	45.8	46.3	69.0	72.6	73.3
26.9	51.2	50.2	50.4	81.8	85.1	86.7
27.0	44.8	44.7	43.4	84.4	88.9	90.5
27.1	42.2	42.6	44.0	83.8	90.2	91.8
27.2	39.1	56.8	57.5	89.4	93.9	94.0
27.3	3.5	4.2	25.2	82.7	91.8	94.6

cally significant increases (at the 98% level) in the explanatory power of the regression analysis. Additionally, raising the order of the polynomial expansion also leads to statistically significant increases in the explanatory power of the larger regression models. Inspection of Table 3 reveals, however, that while the added explanatory power of the third order model is formally statistically significant (due to the large number of samples), the magnitude of the additional variance explained is generally only a slight increase above the second order models.

Figure 4 compares fraction of total variance explained by a quadratic spatial regression analysis with the additional explained variance when temporal expansion terms are included in the quadratic expansion. The spatial-only portion of the analysis explains approximately half of the total variance on all isopycnals within the thermocline with the exception of the deepest surface analyzed ($\sigma_\theta = 27.3$) where it captures only a small fraction of the variance. The inclusion of temporal terms in the polynomial expansion adds marginal explanatory power in the upper portions of the main thermocline but the temporal portion of the signal increases significantly with depth. In the lower main thermocline (e.g., $\sigma_\theta = 27.0$) the time-dependent portion of the signal accounts for roughly half of the total variance of the tritium-^{3}He age observations. The polynomial regression based on a time-dependent Taylor expansion explains over 90% of the variance in the denser isopycnals of the ventilated thermocline. On the densest surface analyzed, $\sigma_\theta = 27.3$, the temporal change in the tritium-^{3}He age signal greatly exceeds the variability in the spatial gradients of the field.

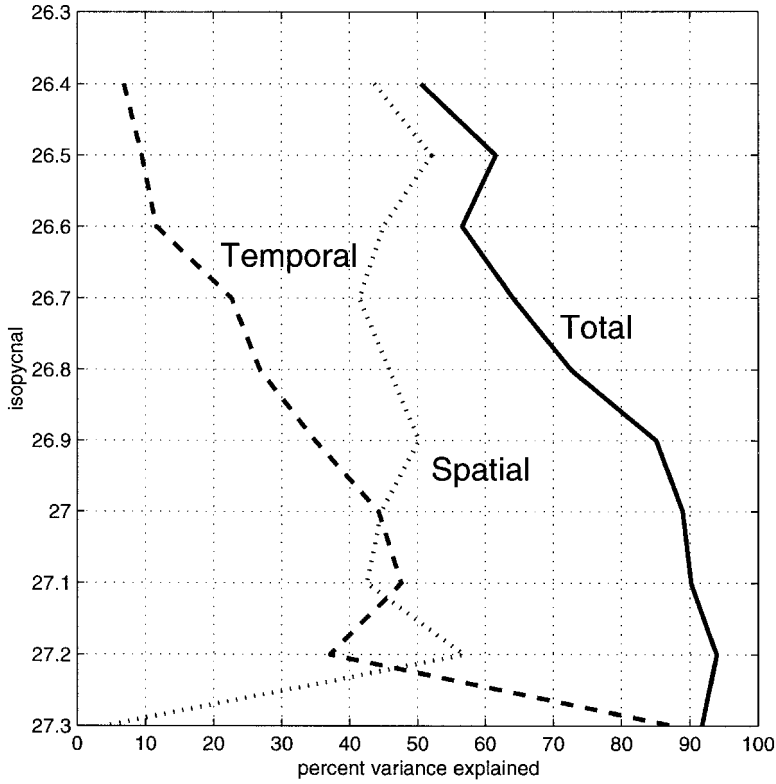

Figure 4. Percent variance explained by regression analysis based on quadratic Taylor expansion of tritium-^{3}He age observations. Solid line is total fraction of variance explained by spatiotemporal model. Dotted line is variance explained with only spatial regressors (e.g., latitude and longitude). Dashed line shows additional percentage of variance when temporal terms are included in expansion.

ii. Determination of expansion parameters across the main thermocline. The regression analysis determines a four-dimensional (density, latitude, longitude, and time) estimate of the structure of the tritium-^{3}He age field in the eastern North Atlantic. Rather than attempt to present a figure of the multidimensional features of the tracer distribution, this section will discuss the key features of the structure of the fields based on interpretation of the diagnosed coefficients of the Taylor expansion of the observations. The coefficients (Fig. 5) of the temporally dependent Taylor expansion (Eq. 4) provide a direct estimate of the spatial and temporal derivatives. The illustrated terms are for an expansion which includes terms quadratic in latitude, longitude and time but is truncated for all higher order terms. The zero-order term (Fig. 5A) represents the mean tritium-^{3}He age in the center of the spatiotemporal domain. The spatial center of the data domain (Fig. 1) is 26N, 30W while the center point in time is chosen to be Jan. 1, 1986. As expected, tritium-^{3}He age increases monotonically with isopycnal (depth) in the thermocline: the mean ages vary from a few

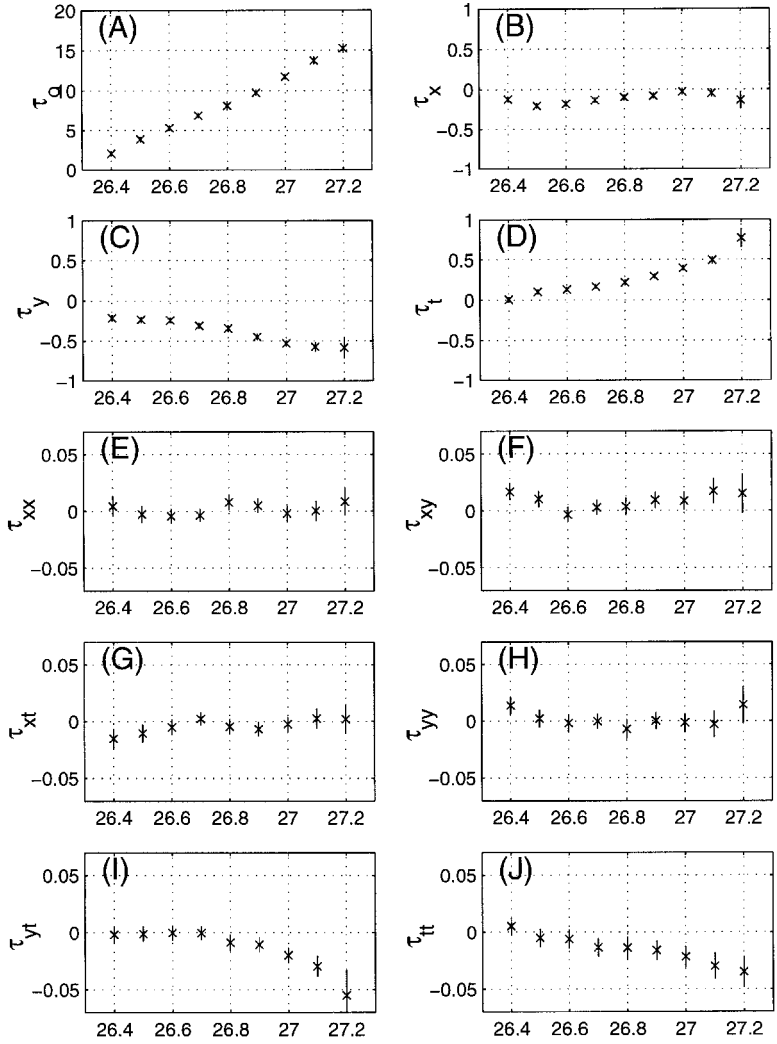

Figure 5. Expansion parameters of temporally dependent Taylor expansion of observed tritium-^{3}He age (yr) distribution on isopycnals determined from multivariate regression analysis centered at 26N, 30W, 1986. Spatial derivative are with respect to degrees of latitude and longitude. Temporal derivatives measure rate of change in years. Thin vertical lines represent the 95% confidence interval for the estimate of each parameter.

years on the lighter surfaces to 15 years at depth. The value of the mean age is well determined by the large number of observations as evidenced by the small size of the 95% confidence interval.

The spatial gradients of age are shown in Figure 5B (zonal gradient) and Figure 5C (meridional gradient). The meridional gradient of age, τ_y, is consistently negative owing to

younger age values toward the north and is in agreement with southward flow away from the location of the isopycnal outcrops into the surface mixed layer. Meridional gradients, τ_y, increase with depth and are stronger than zonal gradients, τ_x. The zonal gradients indicate younger waters toward the east for the lighter density classes and negligible gradients at depth. Taken together, the changes in the first-order spatial gradients as a function of density anomaly are a signature of a counter-clockwise rotation of the gradient of the tritium-^{3}He age field with increasing depth.

The first-order temporal changes in the tritium-^{3}He age field, τ_t, are shown in Figure 5D. The time rate of change of age is significantly positive on all surfaces (except $\sigma_\theta = 26.4$ where it is indistinguishable from zero) with the greatest changes on the densest isopycnals. The magnitude of the temporal trend results in a significant change in the tritium-^{3}He age over the course of the observations. For example, a time rate of change of 0.5 yr/yr produces a change in tritium-^{3}He age of 7.5 years at a fixed point over the fifteen year time span of the observations. Absolute changes of this magnitude have a large impact when the mean ages are of comparable magnitudes (Fig. 5A) and explain why such a large portion of the variance of the observations is in the temporally dependent terms (Fig. 4).

Unlike the first-order terms of the expansion, the quadratic terms are mostly indistinguishable from zero and show less organized structure as a function of density. This is especially true for τ_{xx}, τ_{xy}, τ_{xt}, and τ_{yy} (Figs. 5E, 5F, 5G and 5H, respectively). The terms τ_{yt}, τ_{tt} (Figs. 5I and 5J) do show significant structure distinct from zero, however, and will be discussed in turn.

The second order expansion term, τ_{yt}, can be interpreted as either (A) the time rate of change of the spatial (meridional) gradient of the age field, or (B) the meridional gradient of the temporally dependent portion of the tritium-^{3}He age signal. This term is zero in the upper portion of the main thermocline but gradually increases to significantly negative values for the denser isopycnals. Interpreting this as a temporal change in the meridional gradients of age, which are also negative (Fig. 5C), indicates that the magnitude of the meridional gradients of tritium-^{3}He age are increasing over the time of the observations. These changes are both significantly different from zero and play an important role in altering the first-order gradient: the maximum yearly rate of change on $\sigma_\theta = 27.2$ is about 10% of the magnitude of the meridional gradient in 1986. On the other hand, interpreting the term τ_{yt} as a measure of the spatial structure of the time-dependent portion of the field, negative values indicate that the southern region of the analysis domain is characterized by more rapidly evolving tritium-^{3}He age values.

The second derivative of tritium-^{3}He age against time, τ_{tt} (Fig. 5J), also shows significant negative values which increase with depth in the thermocline. Since τ_t is positive (Fig. 5D), negative values of τ_{tt} indicate that the rate of change of age is decreasing over time. The rate of decrease is greatest on the densest isopycnals where the observed trend in tritium-^{3}He age is largest. The difference in sign of τ_t and τ_{tt} suggests that although the age field is changing over time, the rate of change is slowing and thus the tritium-^{3}He age field may be approaching a steady-state value.

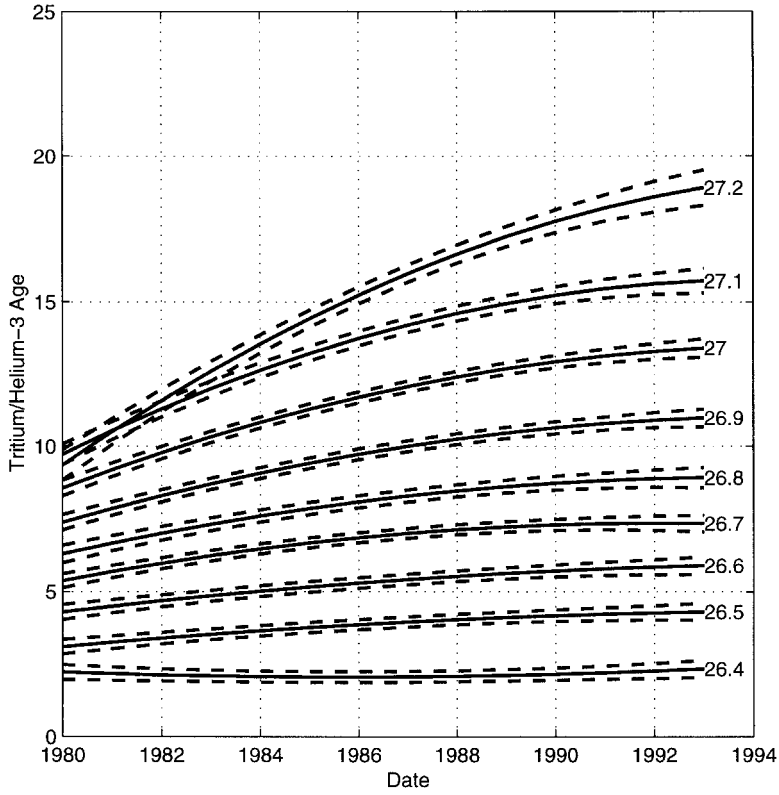

Figure 6. Diagnosed temporal evolution of tritium-^{3}He age on isopycnal surfaces spanning the main thermocline at 30W, 26N. Evolution is determined from multivariate polynomial regression analysis of observations. Dotted lines indicated envelope of standard error of age estimate for each isopycnal surface.

The temporal evolution of the tritium-^{3}He age at the center of the geographic domain is illustrated in Figure 6. At $X, Y = 0$, the curve for each isopycnal shown in Figure 6 is simply determined from

$$\tau = \overline{\tau} + \tau_t T + \tau_{tt} T^2$$

where $\overline{\tau}$, τ_t, and τ_{tt} are the values determined from the regression (Fig. 5) and $T =$ (time $-$ 1986). Many of the characteristics of the tritium-^{3}He age field discussed above are evident (Fig. 6: (A) the increase of tritium-^{3}He age with density, (B) the increase of tritium-^{3}He age over time with near steady state on the lightest densities of the main thermocline and largest changes on the densest surfaces, (C) the decreasing rate of change over time and apparent approach toward a steady state, and (D) increasingly longer relaxation times with depth).

c. Application of multivariate regression model to observed tritium and ^{3}He concentrations

The quantitative interpretation of the tritium-^{3}He age distribution in Section 4 also requires estimates of the spatial gradients of the tritium and ^{3}He on isopycnal surfaces. Diagnosis of the spatial and temporal character of the transient tracer concentrations in the eastern Atlantic is carried out in a similar manner to that of tritium-^{3}He age and will only be discussed briefly here. Estimation of measurement uncertainty, weighting of the multivariate regression and tests for statistical significance are identical to those described in Section 3b. The multivariate regression model based on a Taylor expansion in both space and time (Eq. 4) is applied to the measurements of tritium and ^{3}He concentrations interpolated onto surfaces constant potential density anomaly. Figures 7 and 8 show the expansion coefficients for tritium and ^{3}He, respectively.

Tritium concentrations (Fig. 7A) show a slight increase with depth to a subsurface maximum at $\sigma_\theta = 26.9$ with a steep decrease in concentrations on deeper density surfaces. Spatial gradients (Fig. 7B and 7C) are stronger in the meridional direction than zonal and show the greatest magnitude on the deep surfaces where the concentrations are the lowest. Tritium concentrations are decreasing with time on all the isopycnal surfaces (Fig. 7D) but if the known rate of radiodecay is accounted for, the decay-corrected tritium concentrations on isopycnals $\sigma_\theta \geq 27.0$ are found to be increasing with time. The curvature of the isopycnic tritium distribution (Fig. 7E and 7H) is largest on the densest isopycnals and has greater magnitude in the meridional direction. The time-rate of change of the meridional gradient of tritium (Fig. 7I) is statistically significant and indicates a decrease of the magnitude of the gradient over time. The $\partial^2[^3\mathrm{H}]/\partial t^2$ term is also statically significant but is largely accounted for by radiodecay. Overall, the tritium distribution in the upper thermocline ($\sigma_\theta \leq 26.9$) is nearly homogeneous and decreasing at a rate slightly faster than can be accounted for by radiodecay. In contrast, the tritium in the lower thermocline ($\sigma_\theta \geq 27.0$) is characterized by lower concentrations with steeper diapycnal and isopycnal gradients. Accounting for temporal changes due to radiodecay, the concentrations are increasing with time while the spatial gradients are decreasing. All the diagnosed expansion coefficients in the lower thermocline are consistent with a hypothesis that the effects of peak bomb tritium input signal of the 1960's have yet to fully penetrate onto the denser isopycnal surfaces.

The distribution of ^{3}He shows concentrations increasing with depth (Fig. 8) with a subsurface maximum deeper than that of tritium. Significant spatial gradients are observed both zonally and meridionally (Fig. 8B and 8C) with a rapid reversal of the meridional gradient at the densest isopycnals. With the exception of $\sigma_\theta = 27.2$ the highest ^{3}He are toward the southeast on the lighter surfaces and with rotation toward the south with depth. The meridional curvature of the ^{3}He distribution (Fig. 8H) is significant and also increases with depth. The time-dependent portion of the fields reveals a rich structure with combinations of characteristics changing dramatically as a function of density anomaly.

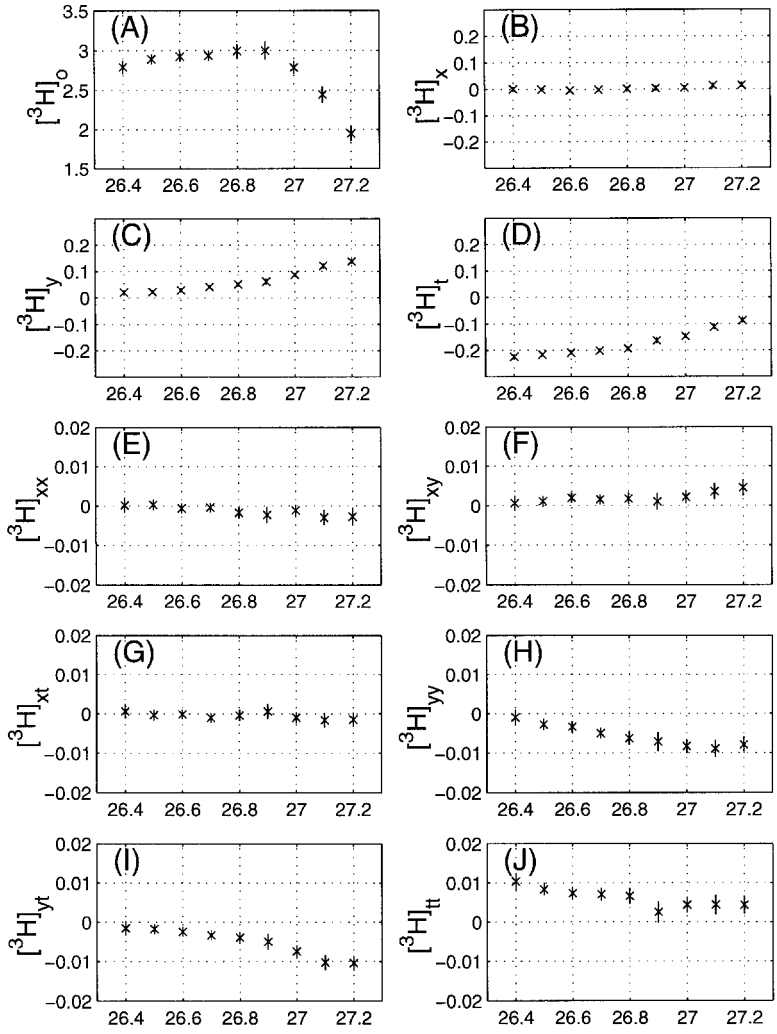

Figure 7. Expansion parameters of temporally dependent Taylor expansion of observed Tritium (T.U.) distribution on isopycnals determined from multivariate regression analysis centered at 26N, 30W, 1986. Spatial derivative are with respect to degrees of latitude and longitude. Temporal derivatives measure rate of change in years. Thin vertical lines represent the 95% confidence interval for the estimate of each parameter.

Concentrations decrease with time in the lighter density classes but increase below $\sigma_\theta = 27.0$. A more thorough interpretation of the ^{3}He distribution requires concurrent analysis of the source function, tritium. Tritium-^{3}He age captures the coupling between the two tracer systems and generally provides a simpler context with which to examine the ^{3}He distributions.

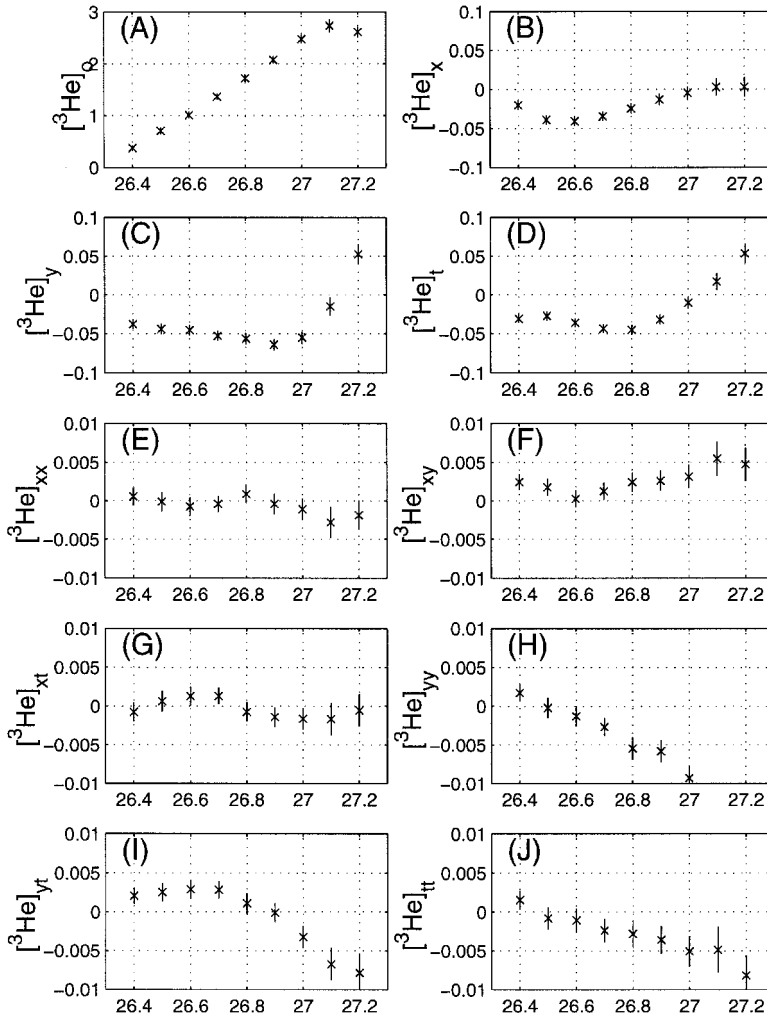

Figure 8. Expansion parameters of temporally dependent Taylor expansion of observed ^{3}He (T.U.) distribution on isopycnals determined from multivariate regression analysis centered at 26N, 30W, 1986. Spatial derivative are with respect to degrees of latitude and longitude. Temporal derivatives measure rate of change in years. Thin vertical lines represent the 95% confidence interval for the estimate of each parameter.

d. Comparison with directly measured trends at Bermuda

The Helium Isotope Laboratory at Woods Hole conducted a time series of ^{3}H and ^{3}He measurements at a hydrographic station near Bermuda (32°10′N, 64°30′W) from 1977 through 1988. Portions of this time series have been previously discussed in terms of thermocline ventilation (Jenkins, 1980; 1982), air-sea gas exchange (Jenkins, 1988a), isopycnal diffusivity (Jenkins, 1991), and the vertical flux of nitrate (Jenkins, 1988b). The

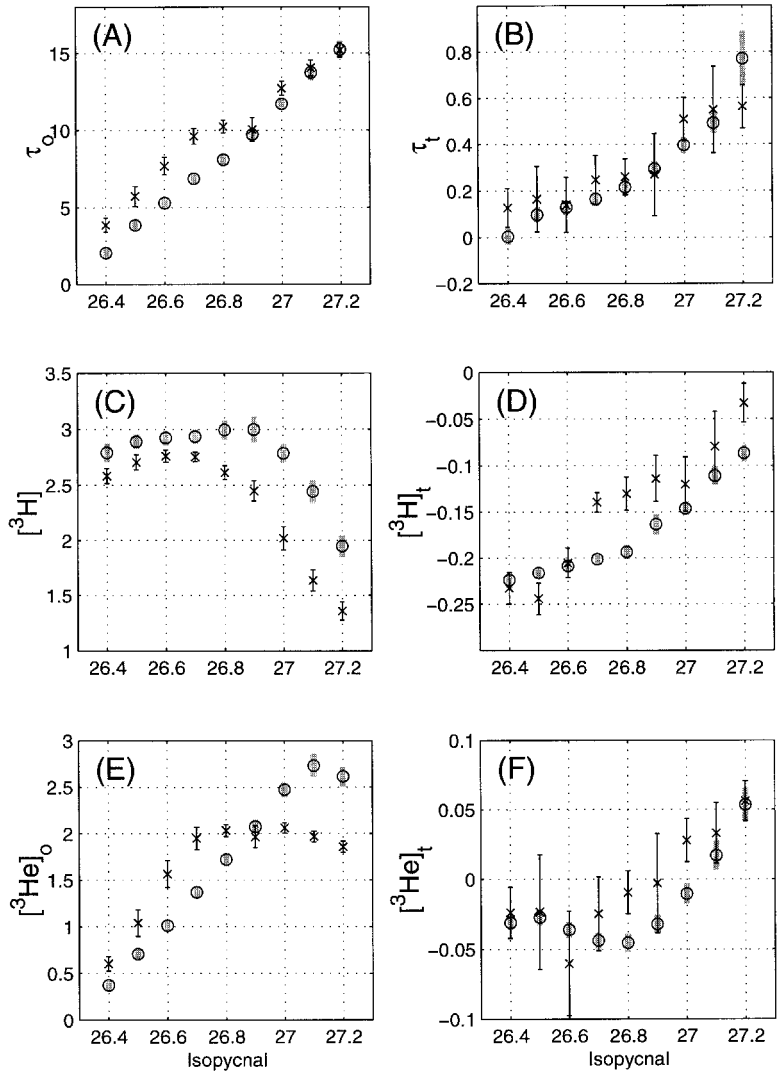

Figure 9. (A) Tritium-^{3}He age and (B) time rate of change of age estimated on isopycnal surfaces at Bermuda for the year 1986. Estimates are based on time-series data between 1976 and 1989 and are indicated by x's. For comparison the estimates of mean age and age tendency in the eastern North Atlantic are indicated by o's. Error bars for both sets of measurements represent the 95% confidence intervals.

hydrographic time series of temperature and salinity at Bermuda is representative of changes throughout the western portion of the subtropical gyre (Joyce and Robbins, 1996; Molinari *et al.,* 1997) which, unlike the eastern North Atlantic, is characterized by strong recirculation from the western boundary current rather than direct ventilation from the surface mixed layer (Luyten *et al.,* 1983; Schmitz and McCartney, 1993).

Figure 9 shows the observed tritium, ^{3}He and tritium-^{3}He age, as well as their rates of change on isopycnals at Bermuda. The tracer measurements at Bermuda are linearly interpolated onto isopycnal surfaces with interpolation errors estimated as previously in the eastern Atlantic. For comparison, the values obtained from the multivariate regression in the eastern Atlantic are also included on Figure 9. On each isopycnal, the tracer age at Bermuda is slightly greater than the value in the eastern Atlantic. The greater observed age at Bermuda is consistent with longer ventilation time associated with increased remoteness from the surface outcrops. The trend of increasing tritium-^{3}He age and age tendency with density is strikingly similar in both the western and eastern regions of the subtropical thermocline. The uncertainties of the estimates at Bermuda are greater due to fewer data points from which the estimate is derived. The general agreement in the two data sets, however, support the finding of a systematic trend in tracer age based on the multivariate regressions in the eastern portion of the gyre and further demonstrates that the observations of temporal change of tritium-^{3}He age in the eastern Atlantic are representative of a pattern extending throughout the subtropical gyre.

Tritium values show similar structure as a function of density in both the western and eastern Atlantic. Concentrations are slightly lower at Bermuda, likely due to the longer ventilation pathways allowing for greater decay of tritium concentration before arriving at Bermuda. The temporal change of tritium is also similar in both regions with the greatest difference being at mid-thermocline where values at Bermuda are not decreasing as rapidly as those in the east. The vertical structure of the ^{3}He concentrations shows greater difference east to west: the subsurface maximum is both weaker and shallower. The rate of change of ^{3}He is surprisingly similar in the two regions with the most significant differences again being at mid-depth. The magnitude of the temporal change in ^{3}He is approximately a factor of 5 less than the change in tritium. That the ^{3}He signal is not changing as rapidly as the tritium is an alternative manifestation of the observation that tritium-^{3}He age is evolving over time.

Unlike the time-series at Bermuda the analysis of transient tracer fields in the eastern Atlantic includes information about the spatial gradients of the tracer fields. The added estimates of the spatial structure of the tritium-^{3}He age field provides critical information to distinguish between possible causes of the observed temporal changes in apparent ventilation age. For instance, it is possible that the temporal changes of tritium-^{3}He age at Bermuda might arise from a shift in the circulation which laterally displaces the large-scale gradients, giving rise to an apparent change in ventilation age at a fixed point. While a time series measurement at one point (e.g., Bermuda) could not be used to test for this hypothesis, such an analysis is feasible using the combined spatial-temporal regression in the eastern North Atlantic.

4. Is the time-dependent tracer age field evidence for a change in the circulation?

Previous examination of chloroflourocarbon (CFC-12) tracer fields in the eastern Atlantic (Doney *et al.,* 1998) have documented temporal differences in the tracer age fields indicating changes in ventilation which appear to be associated with the variability of the

North Atlantic Oscillation (NAO). Talley (1996) has demonstrated decadal variability of subtropical mode water ventilation at Bermuda which also appears connected to the NAO. This section examines if the observed changes in the structure of the tritium-^{3}He age fields in the eastern North Atlantic are an additional record of past interdecadel variability in ocean ventilation.

a. Local balance of tritium-^{3}He age

The advective-diffusive balance of tritium-^{3}He age, derived from the advective diffusive balance of the individual tritium and ^{3}He fields (Jenkins 1987), is:

$$\frac{\partial \tau}{\partial t} = \nabla(\kappa \nabla \tau) - \mathbf{v} \cdot \nabla \tau + 1 + \kappa \left(\frac{\nabla[^3\mathrm{H}]}{[^3\mathrm{H}]} + \frac{\nabla[^3\mathrm{H} + {}^3\mathrm{He}]}{[^3\mathrm{H} + {}^3\mathrm{He}]} \right) \cdot \nabla \tau, \tag{8}$$

where κ is a coefficient of diffusion. This equation represents a local budget for tracer age where the temporal change in tracer age is balanced by advection and mixing. The unity term in Eq. 8 represents the accumulation of age with time while the final term on the r.h.s incorporates nonlinear mixing effects arising from the mixture of waters with differing tracer concentrations.

Eq. 8 can be inverted to solve for the component of the velocity field normal to the gradient of the tracer age field:

$$\mathbf{v} \cdot \hat{\mathbf{n}} = \frac{1 - \dfrac{\partial \tau}{\partial t} + \nabla(\kappa \nabla \tau)}{|\nabla \tau|} + \kappa \left(\frac{\nabla[^3\mathrm{H}]}{[^3\mathrm{H}]} + \frac{\nabla[^3\mathrm{H} + {}^3\mathrm{He}]}{[^3\mathrm{H} + {}^3\mathrm{He}]} \right) \cdot \hat{\mathbf{n}}, \tag{9}$$

where $\hat{\mathbf{n}}$ is the unit vector normal to the isopleths of constant age: $\hat{\mathbf{n}} = \nabla\tau / |\nabla\tau|$. All the terms in Eq. 9 can be evaluated based on the multivariate regression analysis of the tracer fields in Section 3b. Previous analyses (Rooth and Östlund, 1972; Jenkins, 1980; Fine *et al.,* 1981; Sarmiento *et al.,* 1982; Fine *et al.,* 1987) have shown that the diapycnal effects are second order for penetration of transient tracers into the stratified thermocline: the analysis here will be confined to treatment of individual isopycnal surface. The lateral diffusivity, κ, is not determined by the regression analysis and is taken to be spatial homogeneous with a magnitude of 1000 ± 500 m^2 s^{-1} (Bauer and Siedler, 1988; Joyce *et al.,* 1998; Ledwell *et al.,* 1998). The results are not overly sensitive to the choice of lateral diffusivity since the Laplacian of the age field is small (Fig. 5E and H), as is the magnitude of the normalized gradients in the right-hand term of Eq. 8. Figure 10 displays the magnitude of the isopycnal velocity and orientation of the unit normal vector for the density surfaces spanning the thermocline. As expected based on the geostrophic shear, the magnitude of the velocity diminishes with depth: the magnitude of the velocity at $\sigma_\theta = 26.5$ is order 1 cm/s and decreases to order 1 mm/s at $\sigma_\theta = 27.2$. The vector normal to the gradient of the tritium-^{3}He age field points to the southeast in the upper layers of the

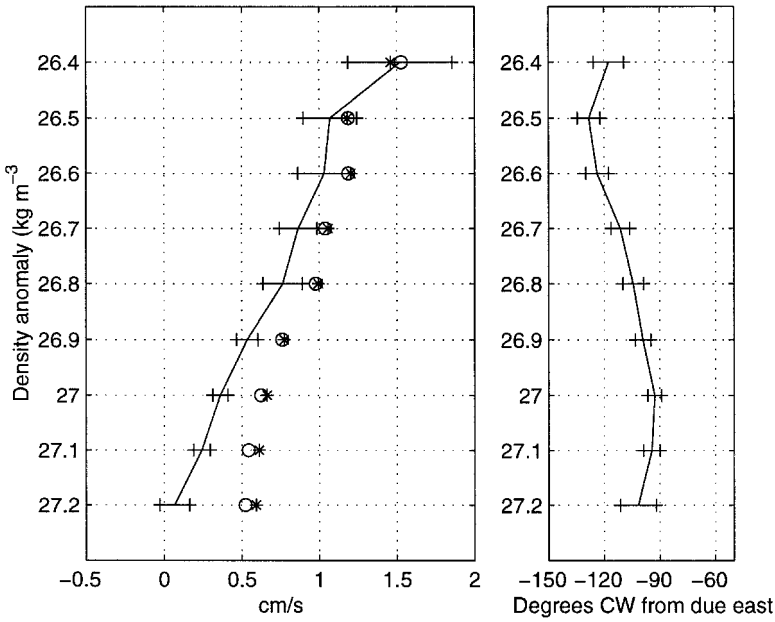

Figure 10. Diagnosed component of isopycnal velocity parallel to gradient of tritium-^{3}He age field: (A) magnitude of velocity and (B) orientation of the gradient of tracer age field. Velocities diagnosed from Eq. 9 are shown as solid line with error bars representing the 95% confidence interval. Confidence intervals are computed based on standard error of the expansion coefficients in Figure 5. Lateral diffusivity is taken to be 1000 ± 500 m^2/s^{-1}. Also shown in panel (A) are two alternative estimates of the velocity field based on truncations of Eq. 9. The '*'s indicate the velocity field computed using the balance: $\mathbf{v} \cdot \hat{\mathbf{n}} = 1/|\nabla\tau|$. Velocities diagnosed using all the terms in Eq. 9 except the time rate of change are shown as 'o's. For clarity, confidence intervals on the latter two estimates are not shown but they are comparable in magnitude to those indicated for the full advective-diffusivebalance.

thermocline and rotates counterclockwise with depth. The orientation of the age isopleths on the denser isopycnals is nearly zonal.

Previous analysis have used similar or simplified versions of Eq. 8 to estimate the local velocity field in the eastern Atlantic thermocline. Roether and Fuchs (1988) argued that both the temporal change term and the mixing terms were small, thereby reducing the dominant balance to $\mathbf{v} \cdot \hat{\mathbf{n}} = 1/|\nabla\tau|$. The velocity estimates based on this simplified balance, repeated here with the present estimate of the tracer gradients, are indicated by the '*'s in Figure 10. In the upper portions of the thermocline, where the temporal changes in the age field are small, the two methods agree reasonably well, however, the discrepancy increases with depth where the relative magnitude of $\partial\tau/\partial t$ becomes significant. Jenkins (1987) included estimates of the diffusive terms (assuming a lateral diffusivity of 500 m^2 s^{-1}) in the local balance but also neglected $\partial\tau/\partial t$ since it could not be determined from data available at the time. The 'o's in Figure 10 indicate the estimates of the normal velocity field based on inclusion of the diffusive terms but neglect of the tendency term. In

agreement with previous work, inclusion of the diffusive mixing terms has the greatest impact on the densest, most slowly ventilated isopycnals but the overall inclusion of diffusive effects results in only minor changes to the estimate of the local velocity field: the 'o's and '*'s are nearly coincident. Jenkins (1998) estimates velocity based on the complete local balance equation. In distinction to the present analysis, Jenkins (1998) determines the spatial gradients only from data collected in 1991–1993 and estimates the $\partial\tau/\partial t$ term based on a simple difference between the observations in the early 1990's and those in the early 1980's. Since the present analysis shows that the rate of change of the age field is slowing over time ($\partial\tau^2/\partial t^2 < 0$; Fig. 5J), the analysis in Jenkins (1998) likely overestimates the magnitude of $\partial\tau/\partial t$ appropriate to the diagnosed advective-diffusive balance for the data collected over the period 1991–1993. The present analysis avoids this complication by using the entire available data set to simultaneously form an estimate of all the terms of the balance equation (Eq. 8) at the center of both the spatial and temporal domain (26N, 30W, 1986). Comparison of the differing estimates of isopycnal velocity in Figure 10 shows that the measurements of the temporal change of the tracer age field are a necessary component to accurately determine the isopycnal velocity on the denser isopycnals in the thermocline.

The primary focus of the present work, however, is not to highlight differences from previous analyses but to examine the long term changes in the tritium and ^{3}He fields as evidence of possible changes in circulation. The local balance of tritium-^{3}He age expressed in Eq. 9 can be differentiated with respect to time:

$$\frac{\partial(\mathbf{v}\cdot\hat{\mathbf{n}})}{\partial t} = -\frac{1}{|\nabla\tau|}\frac{\partial^2\tau}{\partial t^2} + \frac{1}{|\nabla\tau|}\frac{\partial}{\partial t}\nabla(\kappa\nabla\tau) - \frac{\left(1-\dfrac{\partial\tau}{\partial t}+\nabla(\kappa\nabla\tau)\right)}{|\nabla\tau|^2}\frac{\partial|\nabla\tau|}{\partial t} + \frac{\partial}{\partial t}\left(\kappa\left(\frac{\nabla[^3\mathrm{H}]}{[^3\mathrm{H}]}+\frac{\nabla[^3\mathrm{H}+^3\mathrm{He}]}{[^3\mathrm{H}+^3\mathrm{He}]}\right)\cdot\hat{\mathbf{n}}\right). \tag{10}$$

All the terms on the right-hand side of Eq. 10, excepting the magnitude of the lateral diffusivity, can be estimated from the regression analysis of the observed tracer fields. Eq. 10 can therefore be employed to test for the steadiness of the local velocity field over the time of the tritium and ^{3}He observation. It should be noted that this is not a test for changes in ventilation *per se,* but rather an examination of the temporal stability of the velocity field in the region of the tracer measurements. The evaluation of the right-hand side of Eq. 10 is presented in Figure 11 for the isopycnal surfaces spanning the thermocline. The lateral diffusivity is again set 1000 ± 500 m^2 s^{-1}. The third order term, $1/|\nabla\tau|\partial/\partial t\nabla\cdot(\kappa\nabla\tau)$, is neglected: examination of the coefficients of the third order Taylor expansion (not shown) indicate this term is not significantly different from zero on any of the isopycnals. Figure 11 shows the estimates of the change in the local velocity are not distinct from zero for any of the isopycnal surfaces analyzed. That is, the temporal changes in individual components of the tritium-^{3}He age field produce a balance consistent with a steady circulation. The largest contribution to the uncertainty in Figure 11 comes from uncertainty

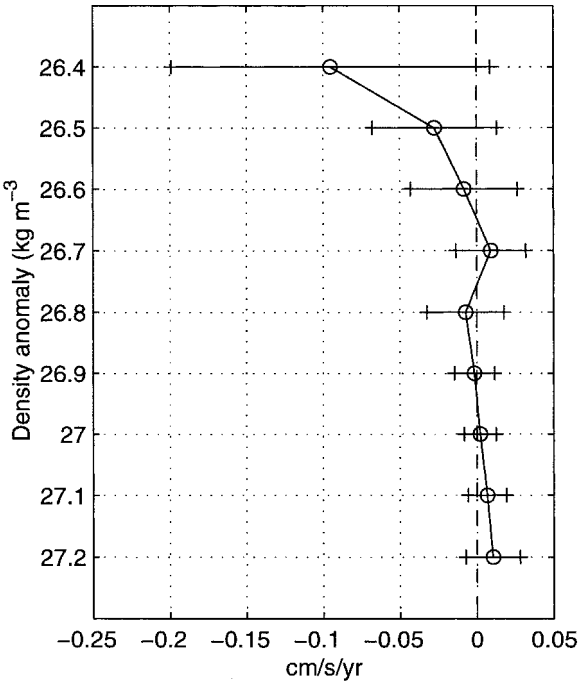

Figure 11. Time rate of change of the velocity field (cm s^{-1} yr^{-1}) as a function of isopycnal surface based on advective diffusive balance of tritium-^{3}He age and diagnosis of spatial and temporal components of tracer fields in the eastern North Atlantic thermocline (Eq. 10). Error bars represent 95% confidence intervals obtained from standard error of diagnosed expansion coefficients and propagation of errors.

in the term proportional to $\partial|\nabla\tau|/\partial t$. Excepting the lightest density surfaces, the upper bound for changes in the large-scale circulation appears to be a few millimeters per second per year.

The analysis summarized in Figure 11 shows that the changes in the tritium-^{3}He age cannot be attributed to changes in the local velocity field but rather are balanced by temporal changes in the magnitude of the local gradient of the tracer age field. This is not to say that the velocity field is constant over the time of the measurements. Rather, on the temporal scales of the data, i.e. a decade, the temporal changes in the magnitude of the tracer age are, to first order, balanced by changes in the local isopycnal gradient of the age field. Examination of the individual terms in Eq. 9 shows that diffusive effects are second order and the primary balance in the tracer age equation is:

$$\frac{\partial\tau}{\partial t} = \mathbf{v}\cdot\nabla\tau + 1. \tag{11}$$

The temporal changes in $\partial\tau/\partial t$ and $\nabla\tau$ occur in concert with a steady velocity, thereby maintaining the overall balance of Eq. 11.

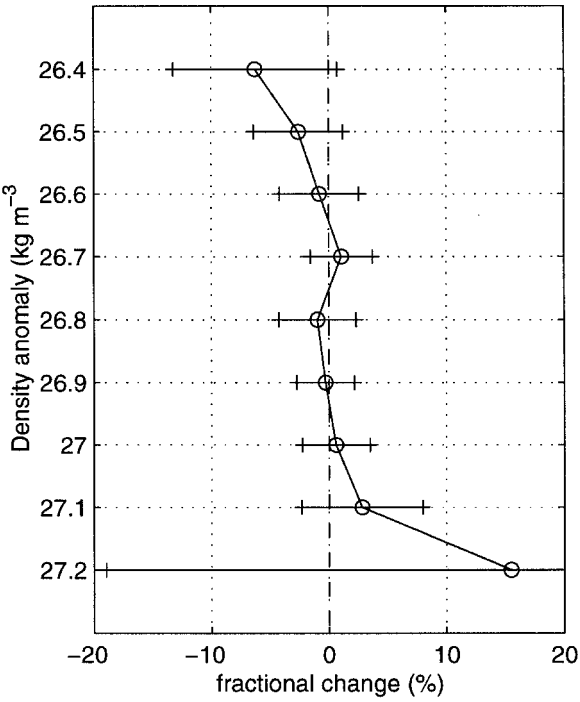

Figure 12. Diagnosed fractional change (per year) in the isopycnal velocity field based on assemblage of tritium and ^{3}He measurements in the eastern Atlantic. A slowing of the local velocity field would result in negative values. Error bars indicate 95% confidence intervals. The right-hand extant of the error bars on the surface $\sigma_\theta = 27.2$ is truncated to allow for greater clarity of the change on other surfaces.

Actual changes in the local velocity field would appear to be a second order effect on the tracer age distribution with the error bars in Figure 11 showing an upper bound on the time rate of change of the large-scale velocity field. The magnitude of this upper bound compared to the mean circulation can be expressed by simply dividing the former by the latter:

$$\Delta = \frac{1}{\mathbf{v}\cdot\hat{\mathbf{n}}}\frac{\partial(\mathbf{v}\cdot\hat{\mathbf{n}})}{\partial t}, \tag{12}$$

where Δ is the fractional change in the velocity field oriented in the direction of the age gradient. Figure 12 shows the calculation of Δ as a function of density anomaly. As implied by the results in Figure 11, the fractional change of the velocity field is not distinct from zero on any isopycnal. The uncertainty of the estimate increases dramatically at the densest isopycnal where the uncertainty in the time of rate of change is comparable to the estimate of the mean velocity. Excepting this surface, the maximum fractional rate of change of the

isopycnal velocity is of order 10% per year with the maximum for most surfaces being less than 5%.

b. Integral balance of tritium-^{3}He age

The previous section examined the observed temporal changes of tritium-^{3}He age in the context of its local advective-diffusive balance. In this section we interpret the changes in the apparent ventilation age in terms of an integral balance of the tracer ventilation. We will focus on two specific questions. Firstly, could the temporal changes in the tracer age be related to possible alterations in the bulk ventilation properties upstream of the location of the tracer observations? Secondly, how does the measured tracer age relate to the true *advective ventilation* time scale?

i. Estimates of changes in bulk ventilation. Since tracer age is always maintained close to zero in the surface mixed layer, the observed age at some position in the shielded thermocline (l) must always be equivalent to an integral of the gradient of the age along the pathways of the flow:

$$\tau(l) = \int_0^l \frac{\partial \tau}{\partial s}\, ds, \tag{13}$$

where the integral represents a line integral along the path of ventilation, s. In general, one does not have observations of the local gradient of the age field all along the path of ventilation. Lacking these observations, the integral may be approximated by assuming the observed isopycnic gradient at position l is representative of its average value upstream (Jenkins, 1987). In this case the relation of Eq. 13 reduces to

$$\tau(l) = l|\nabla\tau|. \tag{14}$$

Differentiating with respect to time yields:

$$\frac{\partial \tau}{\partial t} = \frac{\partial l}{\partial t}|\nabla\tau| + l\frac{\partial|\nabla\tau|}{\partial t}. \tag{15}$$

Eq. 15 shows that changes in age at a fixed point in the thermocline can result from two separate physical processes. The first term on the right-hand side represents changes in the distance to the surface outcrop along the path of the flow. Increases in this distance lead to proportional increases in the observed ventilation age within the thermocline. The second term on the right-hand side captures shifts in the observed age due to temporal changes in the gradient of the age field along the trajectory of the subducted flow. Analysis of the historical record of tritium and ^{3}He measurements in the eastern Atlantic (Section 3b) reveal that the isopycnic gradient of tritium-^{3}He age is steepening over time (Fig. 5G and 5I).

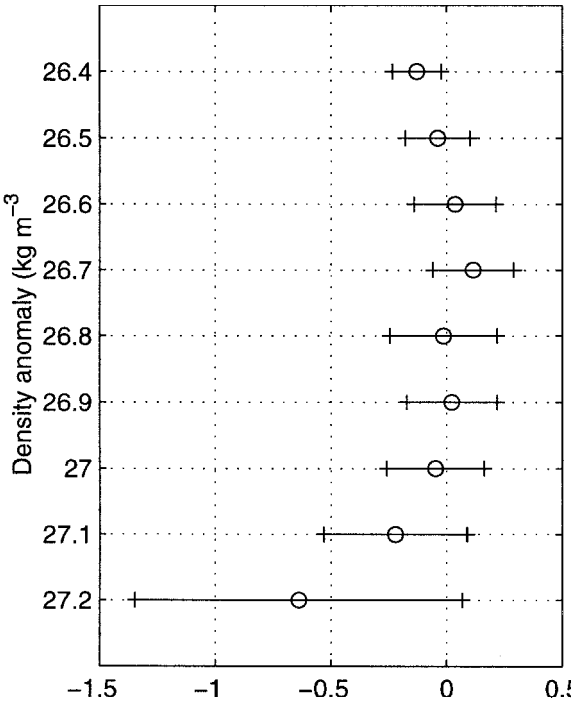

Figure 13. Sum of the two terms on the r.h.s. of Eq. 16 evaluated from the multivariate regression coefficients of tritium-^{3}He age on isopycnal surfaces. Error bars indicate 95% confidence intervals. Estimates which are not distinct from zero show that the observed local change of tritium-^{3}He age is consistent with that expected based on steady ventilation in conjunction with the temporally evolving isopycnal gradient of τ.

Substituting the approximation of Eq. 14 into Eq. 15 and rearranging terms yields:

$$\frac{\partial l}{\partial t}|\nabla\tau| = \frac{\partial \tau}{\partial t} - \frac{\tau}{|\nabla\tau|}\frac{\partial |\nabla\tau|}{\partial t}. \tag{16}$$

In this arrangement all the terms on the right-hand side can be evaluated based on the spatiotemporal regression estimates of the tracer age field. The left-hand side of Eq. 16 cannot be evaluated without independent information on temporal changes in the position of the isopycnal outcrops. Figure 13A displays the evaluation of the right-hand side of Eq. 16 based on the Taylor expansion coefficients in Section 3b. For all but the lightest isopycnal surface, the result is not distinguishable from zero. The two terms on the right-hand side balance each other suggesting that the observed temporal changes in the magnitude of the tritium-^{3}He age field ($\partial\tau/\partial t$; Fig. 5A) are created by the integral effect of the temporally evolving gradient of tracer age on each isopycnal. Analysis of the local balance in the previous section has shown that the temporally evolving gradients are consistent with a locally steady velocity field. The magnitude of $\partial\tau/\partial t$ is decreasing over

time, leading to steeper gradients of tritium-^{3}He age along isopycnals. The results in Figure 13A demonstrate that the observed changes in apparent ventilation age are consistent with the combined integral effects of a steady net ventilation and the observed temporal evolution of the isopycnic gradients of tritium-^{3}He age. For a steady circulation, steeper gradients of age result in greater accumulation of age along the paths of the flow field, the manifestation of which is the apparent increase in tracer age at a fixed point in the thermocline.

Figure 13 shows that a secular change in outcrop position (the left-hand side of Eq. 16) is not necessary in order to explain the observed changes in the tracer age field. It is possible to place an upper bound on the stability of the outcrop positions by dividing Eq. 16 by the gradient of age, yielding an equation for $\partial l/\partial t$ in terms of the observable properties of the tritium-^{3}He age field. The implied stability of the outcrop position is under 100 km/yr for all but the densest isopycnal with some surfaces in mid-thermocline appearing stable to 50 km/yr. Bear in mind that this is not an estimate of the year-to-year variations in outcrop position which may be much greater. The estimate of stability based on the Taylor expansion coefficients of Section 3b represents a bound on the change in position of the time scales of the tracer observations: i.e., a decade.

On the isopycnal surface $\sigma_\theta = 26.4$, the right-hand side of Eq. 13 is not equal to zero within the 95% confidence interval, though the difference is marginal. Comparing the magnitude of this residual to the mean age on the surface suggests a decrease in ventilation of the order 6% per year. Examination of the expansion parameters (Fig. 5) shows that the majority of time dependence on this isopycnal is due to apparent changes in the zonal gradient. Since, this isopycnal outcrops within the domain of the regression analysis we cannot rule out the possibility that the diagnosed temporal changes on this surface result from aliasing of seasonal measurements in the observations.

ii. Estimates of advective ventilation age. The observations and analysis presented thus far present a picture where the tritium-^{3}He age is evolving over time in a manner consistent with a steady ventilation process. Throughout, it has been presumed that the observed tritium-^{3}He age is a first order representation of the true ventilation age. This section develops a more accurate estimate of the true ventilation age based on the observed tracer age and its rate of change. Given the primary balance of the local budget of tritium-^{3}He age (Eq. 11) the integral balance expressed in Eq. 13 can be rewritten as:

$$\int_0^l \frac{\partial \tau}{\partial s}\, ds = \int_0^l \left(\frac{1}{v} - \frac{1}{v}\frac{\partial \tau}{\partial t}\right) ds, \tag{17}$$

$$\tau_{(s=l)} = l\left[\overline{\frac{1}{v}}\right] - \int_0^l \frac{1}{v}\frac{\partial \tau}{\partial t}\, ds, \tag{18}$$

where l is again taken to be the distance along the trajectory of a subducted parcel from the surface outcrop to the point of observation and the overbar represents an average along this path. In general, the right-most term in Eq. 18 cannot be evaluated without measurements of $\partial\tau/\partial t$ along the path of ventilation. However, since the age at the outcrop position is always zero, the time rate of change of age at the outcrop is also zero: $\partial\tau/\partial t_{(l=0)} = 0$. Therefore, applying the trapezoid rule, an approximation of the integral of the tendency term is:

$$\int_0^l \frac{1}{v}\frac{\partial\tau}{\partial t}\,ds \approx \frac{1}{2}\overline{\left[\frac{1}{v}\right]}\frac{\partial\tau}{\partial t_{(s=l)}}. \tag{19}$$

The expression for the integral of the advective-diffusive balance along the path of integration then becomes

$$\tau_{(s=l)} \approx \frac{l}{v_o}\left(1 - \frac{1}{2}\frac{\partial\tau}{\partial t_{(s=l)}}\right). \tag{20}$$

where $1/v_o$ represents the average $\overline{[1/v]}$. This relation can then be inverted to solve for the true advective ventilation age as a function of the locally measured age and its rate of change:

$$\tau_{advective} = \frac{l}{v_o} \approx \frac{\tau_{(s=l)}}{1 - \frac{1}{2}\frac{\partial\tau}{\partial t_{(s=l)}}}. \tag{21}$$

Eq. 21 shows that the true advective age is the product of the observed tritium-^{3}He age and the "correction factor," $1/[1 - (\frac{1}{2})(\partial\tau/\partial t)]$, which partially accounts for the temporal variability of the age field. The magnitude of this "correction factor" ranges from near unity on the lighter isopycnals to 1.6 on $\sigma_\theta = 27.2$.

Figure 14 compares the two estimates of ventilation age (observed tritium-^{3}He age versus advective age based on Eq. 21) on a representative isopycnal surface. The ventilation age implied by the observed tracer concentration is shown in Figure 14A while Figure 14B displays the estimate corrected for the observed time rate of change in age assuming the approximated first order advective-diffusive balance in Eq. 11. At all locations, the estimate of the advective age exceeds the observed tracer age by a significant amount. The magnitude of the difference on $\sigma_\theta = 26.8$ varies from about 8% to 20% with the largest difference at the oldest ages. The resulting estimate of advective age shows a stronger gradient along the isopycnals than the observed age, consistent with the results of the local analysis which show the accumulation of tritium-^{3}He age following a parcel is balanced by both the velocity up the age gradient as well the local rate of change in tracer age.

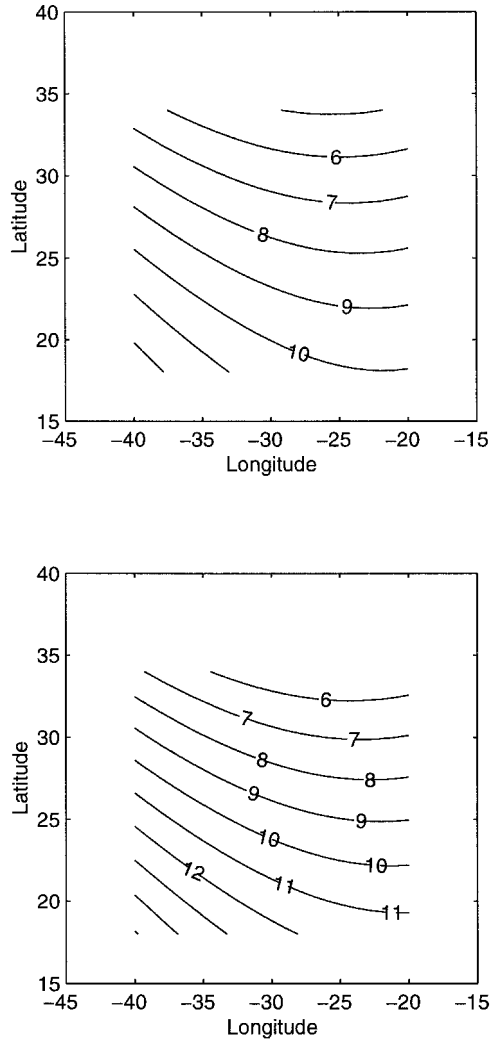

Figure 14. Contour plots of tritium-^{3}He age (yrs) on the isopycnal $\sigma_\theta = 26.8$ based on application of multivariate regression analysis to observations in region. (A) Tracer age in 1986, (B) Estimate of true advective ventilation age based on observed rate of change of tritium-^{3}He age and Eq. 21.

5. Summary

For this paper we have analyzed 15 years of tritium and ^{3}He measurements in the eastern North Atlantic thermocline with specific emphasis on the temporal behavior of the tracer age field. Contrary to expectations that the age field would be nearly steady with time in this well ventilated region (Thiele and Sarmiento, 1990; Roether, 1989), regression of the observations in a spatial-temporal Taylor expansions yields significant trends of tritium-^{3}He age with time. The tritium-^{3}He age increases over time with the structure of the change

varying smoothly with depth and position. The largest temporal changes of the tritium-^{3}He age field are found in the oldest waters. The trends in tracer age in the eastern Atlantic are similar to those directly observed at Bermuda, however, unlike the time series of measurements at Bermuda (Jenkins, 1980; 1982; 1991), the analysis in the eastern Atlantic estimates both temporal changes and spatial gradients. Because of the additional information about the spatial structure of the tracer age field, several hypothesis of the cause of the temporal changes can be examined.

The temporal change in tritium-^{3}He age in the eastern Atlantic can be interpreted within the context of two distinct balances. The first, a local advective-diffusive balance, is dependent on the isopycnic velocity field in the region of the tracer observations. The second, an integral balance, quantifies the ventilation time scale of the domain between the region of tracer observations and the surface outcrop location of each isopycnal.

The local advective-diffusive balance of tracer age can be inverted to solve for the component of the velocity field in the direction of the age gradient. As observations of tritium and ^{3}He have accumulated, investigators have been able to diagnose more terms in the overall balance allowing for more refined estimates of the velocity field (Jenkins, 1987; Roether and Fuchs, 1988; Jenkins, 1998). The present work, agreeing with the previous studies, finds that the effects of diffusive mixing play a relatively minor role in the local advective-diffusive balance of tritium-^{3}He age in the 1980's. In contrast, the temporal tendency, $\partial\tau/\partial t$, is a significant term in the balance, especially in the lower thermocline. Prior studies neglecting the temporal effects have lead to overestimates of the isopycnal advection on the denser isopycnals in the eastern North Atlantic. An expression for the rate of change of the local velocity field is formed by differentiating the local advective-diffusive balance with respect to time (Eq. 10). This equation relates changes in the large-scale structure of the age, tritium and ^{3}He fields to changes in the local velocity. The temporal evolution of the structure of tracer fields are diagnosed by the multivariate regression analysis in Section 3b and found to be consistent with the local velocity field which is steady over the period of the observations (Fig. 11).

In contrast to the local advective-diffusive balance, the observed magnitude of the tracer age is a function of the integral of the tracer evolution along the pathways of ventilation. Analysis of the local balance has shown that the gradients of the tracer age have evolved in a manner consistent with a steady local velocity. Extrapolation of the time-dependent tracer gradients to the isopycnal surface outcrops (Jenkins, 1987) reveals that the temporally evolving tritium-^{3}He age also shows consistency with steady ventilation over the larger domain: as the isopycnic gradients in the tritium-^{3}He age increase over time, the observed tracer age at a fixed point must likewise increase.

Though the observation of tritium-^{3}He age provides a first-order estimate of the ventilation time scales of the thermocline, the temporally evolving character of the fields indicates that second order effects can lead to significant biases in this estimate, especially in the lower thermocline. An integral balance accounting for the temporal effects yields a more refined estimates of the true advective ventilation age as a function of the observed

tracer age and its rate of change (Eq. 21). The improved estimates show general agreement with the observed tritium-^{3}He age in the upper thermocline where the tracer age field is steady. In the lower thermocline, however, the observed tritium-^{3}He age underestimates the actual ventilation by up to 40%. The magnitude of this bias is decreasing over time suggesting that observations of tritium-^{3}He age taken in the 90's will yield closer estimates to the true ventilation age.

Why does the tritium-^{3}He age evolve over time if the circulation field is, as deduced, actually steady over the time scales of the observation? Simple models of the ventilation of tritium and ^{3}He (Jenkins, 1980; Robbins, 1997) are characterized by large changes in the tritium-^{3}He age in response to the sudden input of bomb produced tritium to the surface ocean in the 1960's. The sudden invasion of tritium into the youngest waters of the thermocline leads to decreases in the tritium-^{3}He age with respect to the true ventilation age. Numerical simulations suggest that the proximate cause to this bias is the action of the nonlinear mixing effects (right-hand term of Eq. 9) acting on the very steep spatial gradients of the tritium and ^{3}He concentrations. Over time, as the tritium inventory becomes more homogenized, the relative importance of non-linear mixing term decreases and the tritium-^{3}He age begins to increase as it relaxes back toward values consistent with the true ventilation age. The observations of tritium-^{3}He age in the eastern Atlantic thermocline capture the only the latter period when the tritium-^{3}He age is increasing in value. The nonlinear mixing terms have largely decreased in importance by this time, though their early significant effects remain "fossilized" in the observed large temporal changes in the tracer age field.

The present work is in contrast to the findings of (Doney *et al.,* 1998), who deduced large changes in ventilation in the eastern Atlantic thermocline (up to 200%) based on CFC measurements separated by 5 years. Several possibilities may explain the different conclusions reached here. Firstly, the time scales of the analysis differ: The Doney *et al.* (1998) analysis is based on two hydrographic surveys occupied in 1988 and 1993. The present analysis, based on data from 1978 through 1993, focuses primarily on the changes over this longer time scale. Secondly, the results suggesting large changes are based on ventilation age determined from observed CFC partial pressure. While the ventilation age determined from the differing transient tracer systems shows general agreement for ages less than 15 years (Doney *et al.,* 1997), the temporal character of the surface boundary conditions are quite different: surface tritium increased suddenly in response to atmospheric bomb tests in the early 1960's while the atmospheric burden of CFC's has ramped up more slowly over time. The observed temporal changes of the tritium-^{3}He age field are largely a response to the sudden step-like increase in surface tritium concentrations in the 1960's. Changes in the ventilation rate will also impact the tracer distributions but the present analysis has not been able to resolve such possible alterations. Age estimates based on CFC concentrations should show less temporal change in response to the changes in the surface boundary condition and are therefore, more likely to be sensitive to interannual changes in ventilation processes. Finally, the conclusions of Doney *et al.* (1998) are based

on the simple difference in magnitude of tracer age at two points in time. The analysis of this paper, specifically in Section 4b, shows that changes in apparent tracer age can arise from the subtle interplay between advection against the age gradient and the local time rate of change. Properly accounting for temporal changes in the gradients of the age field appears to be required for interpretation of changes in the large scale distribution of tracer age.

We have examined a compilation of transient tracer observations in the eastern North Atlantic. A spatial-temporal regression analysis reveals large, statistically significant changes in the tritium-^{3}He age field. While these changes may at first seem to be evidence of long-term changes in thermocline ventilation, the analysis presented in this paper shows that, to first order, the temporal changes in tracer age arise from the details of the time-dependent local balance of the tracer age and are consistent with a steady rate of large-scale ventilation. While measurements of transient tracers offer a unique opportunity to directly observe the ventilation of the ocean, care is required in the quantitative interpretation of the apparent age determined from the tracer concentrations. The present study has not concluded that interannual or interdecadel variability in oceanic ventilation cannot be detected from measurements of tritium-^{3}He age. Rather, the observed decadal changes of the tritium-^{3}He age field in the North Atlantic are primarily a response to the time-dependent invasion of bomb-tritium into the thermocline. Understanding and quantifying this intrinsic component of the temporal structure of the transient tracer fields is a prerequisite step for using transient tracers as indicators of temporal changes in oceanic ventilation.

Acknowledgments. The majority of this work was conducted while the first author was a graduate student in the MIT/WHOI Joint Program in Oceanography. PER thanks his thesis advisors, Jim Price and Breck Owens, for their support, encouragement and advice throughout this project. The high quality database of ^{3}He and tritium measurements is the result of many years of dedicated collection and measurement by members of the Helium Isotope Laboratory at Woods Hole: D.E. Lott, M.W. Davis, S.P. Birdwhistell, J.M. Curtis, M.O. Mathewson and P.B. Landry. Critical remarks by R. Pickart and two anonymous reviewers lead to a more concise presentation of this material. This research was supported by Office of Naval Research ASSERT contract number N00014-95-1. ^{3}H and ^{3}He measurements were supported by ONR Grant N00014-90-J-1384 as well as numerous NSF grants. This is WHOI contribution no. 9667.

APPENDIX

Statistical tests of optimum least squares solutions

The ability of a multivariate regression model to explain a set of data can be measured quantitatively by examining the magnitude of the residuals between data and the model predictions. The typical measure is the sum of the squares of the residuals, *RSS:*

$$RSS = \sum (\mathbf{E}m - \tau). \tag{22}$$

For a weighted-least squares solution this value must be normalized by the uncertainty of the data:

$$RSS = \sum \frac{(\mathbf{E}m - \tau)}{\sigma_\tau}. \tag{23}$$

In general, adding more regressor variables, in this case increasing the order of the polynomial fit, will always decrease the value of *RSS*. It is crucial to differentiate between a decrease in *RSS* created by an improvement in the model structure as opposed to a decrease in *RSS* due simply to a decrease in the degrees of freedom of the model. To determine if this improvement in the model fit is statistically significant, the *RSS* of two models can be compared with an *F*-statistic:

$$F = \frac{\dfrac{RSS_0 - RSS_1}{p_1 - p_0}}{\dfrac{RSS_1}{N - p_1}} \tag{24}$$

where the subscripts represent the two models, p is the number of regressors for each model and N is the total number of data points. In this case the value of p_1 is greater than p_0 indicating that model 1 has more regressor coefficients than model 0. The denominator of Eq. 24 is a measure of the variance of the model with the greater number of regressor variables. The numerator is the reduction in variance of the more complex model compared to the simpler model. A large *F*-value indicates that the higher order model leads to a substantial reduction in the variance of the residuals. The critical value for a statistically significant reduction of variance is a function of N, p_1, p_0 and a desired confidence level. *F*-tests are used in this analysis as a criterion of the ability of differing regression models to fit the observed age measurements.

REFERENCES

Anderson, T. W. 1984. The 1982 Wald Memorial Lectures: Estimating Linear Statistical Relationships. The Annals of Statistics, *12,* 1–45.

Armi, L. and H. Stommel. 1983. Four views of a portion of the North Atlantic Subtropical Gyre. J. Phys. Oceanogr., *13,* 828–857.

Bauer, E. and G. Siedler. 1988. The relative contributions of advection and isopycnal and diapycnal mixing below the subtropical salinity maximum. Deep-Sea Res., *35,* 811–837.

Böning, C. W. 1988. Characteristics of particle dispersion in the North Atlantic: an alternative interpretation of SOFAR float results. Deep-Sea Res., *35,* 1379–1385.

Doney, S. C., J. L. Bullister and R. Wanninkhof. 1998. Climatic variability in ocean ventilation rates diagnosed using chloroflourocarbons. Geophys. Res. Lett., *25,* 1399–1402.

Doney, S. C., W. J. Jenkins and J. L. Bullister. 1997. A comparison of ocean tracer dating techniques on a meridional section in the eastern North Atlantic. Deep-Sea Res., *44,* 603–626.

Doney, S. C., W. J. Jenkins and H. G. Östlund. 1993. A tritium budget for the North Atlantic. J. Geophys. Res., *98,* 18069–18081.

Dreisigacker, E. and W. Roether. 1978. Tritium and ^{90}Sr in North Atlantic surface waters. Earth Planet. Sci. Lett., *38,* 301–312.

Fine, R. A., W. H. Peterson and H. G. Östlund. 1987. The penetration of tritium into the tropical Pacific. J. Phys. Oceanogr., *17,* 553–564.

Fine, R. A., J. L. Reid and H. G. Östlund. 1981. Circulation of tritium in the Pacific Ocean. J. Phys. Oceanogr., *11,* 3–14.

Fuchs, G. 1987. Ventilation der Warmwassersḧare des Nordostatlantiks Abgeleitet aus ^{3}Helium-und Tritium-Verteilungen, Institut Für Umweltphysik, University of Heidelberg, Doctoral Dissertation.

Isemer, H.-J. and L. Hasse. 1987. The Bunker Climate Atlas of the North Atlantic Ocean, Volume 2: Air-Sea Interactions, Springer-Verlag, NY.

Jenkins, W. J. 1980. Tritium and ^{3}He in the Sargasso Sea. J. Mar. Res., *38,* 533–569.

—— 1982. Oxygen utilization rates in the North Atlantic subtropical gyre and primary production in oligotrophic systems. Nature, *300,* 246–248.

——1987. ^{3}H and ^{3}He in the beta triangle: observations of gyre ventilation and oxygen utilization rates. J. Phys. Oceanogr., *17,* 763–783.

—— 1988a. The use of anthropogenic tritium and helium-3 to study subtropical gyre ventilation and circulation. Phil. Trans. R. Soc. Lond. A., *325,* 43–61.

—— 1988b. Nitrate flux into the euphotic zone near Bermuda. Nature, *331,* 521–523.

—— 1991. Determination of isopycnal diffusivity in the Sargasso Sea. J. Phys. Oceanogr., *21,* 1058–1061.

—— 1998. Studying thermocline ventilation and circulation using tritium and ^{3}He. J. Geophys. Res., *103,* 15,817–15,831.

Jenkins, W. J. and W. B. Clarke. 1976. The distribution of ^{3}He in the western Atlantic Ocean. Deep-Sea Res., *23,* 481–494.

Joyce, T. M. and W. J. Jenkins. 1993. Spatial variability of subducting water in the North Atlantic: a Pilot Study. J. Geophys. Res., *98,* 10111–10124.

Joyce, T. M., J. R. Luyten, A. Kubryakov, F. B. Bahr and J. S. Pallant. 1998. Meso- and large-scale structure of subducting water in the subtropical gyre of the eastern North Atlantic Ocean. J. Phys. Oceanogr., *28,* 40–61.

Joyce, T. M. and P. Robbins. 1996. The long-term hydrographic record at Bermuda. J. Climate, *9,* 3121–3131.

Klein, B. and G. Siedler. 1989. On the origin of the Azores Current. J. Geophys. Res., *94,* 6159–6168.

Ledwell, J. R., A. J. Watson and C. S. Law. 1998. Mixing of a tracer released in the pycnocline of a subtropical gyre. J. Geophys. Res. (in press).

Lozier, M. S., W. B. Owens and R. G. Curry. 1995. The Climatology of the North Atlantic. Prog. Oceanogr., *36,* 1–44.

Luyten, J. R., J. Pedlosky and H. Stommel. 1983. The ventilated thermocline. J. Phys. Oceanogr., *13,* 292–309.

Marshall, J. C., A. J. G. Nurser and R. G. Williams. 1993. Inferring the subduction rate and period over the North Atlantic. J. Phys. Oceanogr., *23,* 1315–1329.

Menke, W. 1984. Geophysical Data Analysis: Discrete Inverse Theory, Academic Press, San Diego, CA.

Molinari, R. L., D. A. Mayer, J. F. Festa and H. F. Bezdak. 1997. Multiyear variability in the near-surface temperature structure of the midlatitude western North Atlantic Ocean. J. Geophys. Res., *102,* 3267–3278.

Musgrave, D. 1990. Numerical studies of ^{3}H and ^{3}He in the thermocline. J. Phys. Oceanogr., *20,* 334–373.

Robbins, P. E. 1997. The Temporal Evolution of Tritium-^{3}He Age in the North Atlantic Subtropical Thermocline, Doctoral Dissertation, MIT/WHOI Joint Program in Oceanography, Cambridge, MA.

Roether, W. 1989. On oceanic boundary conditions for tritium, on tritiugenic ^{3}He, and on the tritium-^{3}He age concept, *in* Oceanic Circulation Models: Combining Data and Dynamics, D. L. T. Anderson and J. Willebrand, eds., Kluwer Academic Publishers, Boston, 377–407.

Roether, W. and G. Fuchs. 1988. Water mass transport and ventilation in the northeast Atlantic derived from tracer data. Phil. Trans. R. Soc. Lond. A., *325,* 63–69.

Rooth, C. G. H. and H. G. Östlund. 1972. Penetration of tritium into the Atlantic thermocline. Deep-Sea Res., *19,* 481–492.

Sarmiento, J. L., C. G. H. Rooth and W. Roether. 1982. The North Atlantic tritium distribution in 1972. J. Geophys. Res., *87,* 8047–8056.

Schmitz, W. J. and M. S. McCartney. 1993. On the North Atlantic circulation. Rev. Geophys., *31,* 29–49.

Siedler, G., A. Kuhl and W. Zenk. 1987. The Madeira Mode Water. J. Phys. Oceanogr., *17,* 1561–1570.

Stammer, D. and C. W. Böning. 1996. Generation and distribution of mesoscale eddies in the North Atlantic Ocean, *in* The Warmwatersphere of the North Atlantic, W. Krauss, ed., Gebrüder Borntraeger, Berlin, 159–193.

Talley, L. D. 1996. North Atlantic circulation and variability. Physica D, *98,* 625–646.

Thiele, G. and J. L. Sarmiento. 1990. Tracer dating and ocean ventilation. J. Geophys. Res., *95,* 9377–9391.

Unterweger, M. P., B. M. Coursey, B. M. Schima and W. B. Mann. 1980. Preparation and calibration of the 1978 National Bureau of Standards Tritiated Water Standards. Int. J. Appl. Rad. Isot., *31,* 611–614.

Warner, M. J., J. L. Bullister, D. P. Wisegarver, R. H. Gammon and R. F. Weiss. 1996. Basin-wide distributions of chloroflourocarbons CFC-11 and CFC-12 in the North Pacific: 1985–1989. J. Geophys. Res., *101,* 20525–20542.

Weiss, R. E., J. L. Bullister, R. H. Gammon and M. J. Warren. 1985. Atmospheric chloroflouomethanes in the deep equatorial Atlantic. Nature, *314,* 608–610.

Worthington, L. V. 1959. The 18 degree water in the Sargasso Sea. Deep-Sea Res., *5,* 297–305.

Wunsch, C. 1988. An eclectic Atlantic Ocean circulation model. II. Transient tracers and the ventilation of the eastern basin thermocline. Phil. Trans. R. Soc. Lond. A, *325,* 201–236.

Received: *29 December, 1997;* revised: *11 June, 1998.*